**Title:** Impacts of changing ocean circulation, temperature, and food supply on larval recruitment of purple sea urchins in Southern California: A biophysical modeling study

**Authors:** Rachel D. Simons[1*] and Daniel K. Okamoto[2]

[1*] Earth Research Institute, University of California, Santa Barbara, CA, USA

[2] Department of Integrative Biology, University of California, Berkeley, CA, USA

[*] Corresponding Author. Address: Email address: simons@eri.ucsb.edu

**Abstract:**

We evaluate the impact of changing ocean conditions on larval recruitment of purple sea urchins in the Southern California Bight using 3D biophysical modeling with temperature, surface chlorophyll, and recruitment data. The influence of circulation, temperature, and food supply on larval recruitment is quantified using modeled variables, which include larval dispersal distance, larval source location, larval food supply, and temperature exposure for larvae and adults and are derived for 18 years and five larval recruitment sites. Sensitivity testing of the variables to different plankton larval durations (PLDs), larval behaviors, and nearshore retention is performed. All variables are found to be relatively insensitive to changes in PLD greater than 26 days. Larval dispersal distance and source location, representing changes in circulation, are found to be more sensitive to larval behavior and nearshore retention than larval food supply and temperature exposure for larvae or adults. All variables are statistically compared to recruitment field data. Temperature exposure for adults during the fall reproductive season is found to be a strong driver of larval recruitment, but temperature exposure for larvae during the spring recruitment season is not. Thus, we hypothesize that the timing of species recruitment and reproduction is a critical factor in predicting the impact of temperature on larval recruitment. Circulation is found to be a driver of larval recruitment if larvae have behavior that reduces their dispersal distance, allowing them to come from source sites near to the recruitment sites. Food supply is not found to be a driver of larval recruitment.

## 1.0 Introduction

Extreme changes in ocean conditions, such as temperature, circulation, and primary productivity, pose significant threats to marine ecosystems and are predicted to alter the distribution and productivity of marine species, in part by affecting larval recruitment (Doney et al. 2012; Sydeman et al. 2014). Improving our understanding of larval recruitment can explain and predict shifts in the dynamics of populations of fished and ecologically important species (Botsford et al. 1998; Myers 1998; Pineda et al. 2010; Stige et al. 2013). Thus, quantifying how ocean conditions shape spatial and temporal variation in larval dispersal and recruitment is critical to our understanding how climate drivers influence marine populations. In this study, we explore the impacts of changing ocean conditions on larval recruitment by investigating the relationship between larval recruitment of purple sea urchins and ocean conditions of circulation, temperature, and food supply in the Southern California Bight (SC Bight, Figure 1) using 3D biophysical modeling.

The SC Bight, the southern component of the California Current System, is a highly volatile transition zone lying at the interface between two very different oceanographic regimes, the cold nutrient-rich waters of the south-flowing California Current and the warm nutrient-poor equatorial waters of the north-flowing Southern California Countercurrent (Lynn and Simpson 1987; Hickey 1993; Winant et al. 2003; Dong et al. 2009). The meeting of these two regimes in the SC Bight creates a year-round temperature gradient with colder water in the north and warmer water in the south and a seasonal chlorophyll gradient with high levels in the north and low levels in the south during the spring and early summer (Otero and Siegel 2004; Henderikx Freitas et al. 2017; Simons and Catlett 2023). As a result, the SC Bight is particularly

sensitive to shifts in the California Current, which can create dramatic changes in ocean circulation, temperature, and primary productivity in the SC Bight and are often correlated with ENSO events (Lynn and Bograd 2002; Dong et al. 2009). Thus, making the SC Bight an ideal system for studying the relationship between changing ocean conditions and larval recruitment.

In the California Current, changes in populations of the purple sea urchin, *Strongylocentrotus purpuratus,* indirectly regulates the species assembly of nearshore rocky coastlines through voracious herbivory on kelp (Tegner and Dayton 1991; Filbee-Dexter and Scheibling 2014). A substantial body of research describes how predation and disease impact adult sea urchin populations (Mann and Breen 1972; Estes and Duggins 1995; Lafferty 2004; Filbee-Dexter and Scheibling 2014) and documents climate-related booms and busts of purple urchins along the California Coast in recent years (Rogers-Bennett and Catton 2019; Okamoto et al. 2020; Rogers-Bennett and Okamoto 2020; Shanks et al. 2020). However, despite the widespread recognition of the importance of larval transport and recruitment in controlling population fluctuations in many marine species (Morgan 2001; Underwood and Keough 2001; Pineda et al. 2007; White et al. 2019), no studies have been conducted that evaluate how changes in ocean conditions influence larval recruitment of purple urchins in the California Current. The purple sea urchin (*S. purpuratus*) is used for this study because long-term, spatially replicated recruitment data is available at six locations in the SC Bight and prior work suggests that high temperatures and ENSO events in the SC Bight are linked to poor recruitment years (Okamoto et al. 2020).

The main goal of this study is to assess the impacts of changes in circulation, temperature and food supply on larval recruitment of purple sea urchins in the SC Bight. A

biophysical model of the SC Bight, an ocean circulation model with particle tracking, is used to estimate larval recruitment at the recruitment sites where long-term urchin recruitment data has been collected (Figure 1, Okamoto et al. 2020). To simulate larval transport to the recruitment sites, the biophysical model is run in reverse time with particles released from the recruitment sites and tracked backwards in time to their spawning location or source site. Source sites in the SC Bight are identified by the presence of potential urchin habitat, which is rocky reef substrate. Using the particle tracking data, temperature from the ocean circulation model, and surface chlorophyll from satellite data, the impact of changing circulation, temperature, and food supply on larval recruitment is quantified by deriving five variables, termed "ocean conditions", for each recruitment site. Two ocean conditions represent circulation, larval dispersal distance (LDD) and source zone strength (SZS). LDD is the distance a particle travels from a source site to a recruitment site. SZS is the relative probability that larvae would originate from nine coastal zones in the SC Bight (Figure 1). Two ocean conditions represent temperature, larval temperature ($T_L$) and source site temperature ($T_S$). $T_L$ is the temperature that larvae are exposed to as they are transported from the source sites to the recruitment sites. $T_S$ is the temperature that adult urchins are exposed to at the spawning or larval source sites during gametogenesis. One ocean condition represents the food availability (Chl), which is estimated using surface chlorophyll concentrations from satellite data along the particle tracks. The five ocean conditions are calculated for an 18-year modeling period from 1996-2013.

To accurately model larval transport and recruitment, the larval life history of the species must be realistically represented in the biophysical model (Paris et al. 2007; Cowen and

Sponaugle 2009; Metaxas and Saunders 2009). However, empirical data on larval life history traits, such as vertical migration behavior, of many species is not available, and thus many studies do not include species-specific larval life history when modeling larval transport and connectivity (Swearer et al. 2019). To address this problem, we evaluate the sensitivity of the five ocean conditions to variations in three larval life history parameters, plankton larval duration (PLD), larval behavior, and nearshore retention. Two types of PLD are simulated, a PLD of 42 days, which is based literature values for purple sea urchins, and a temperature dependent PLD based on experimental studies (Mustermann et al. 2025). Two types of larval behavior are simulated passive drifting and diel vertical migration, which occurs when the larvae migrate to the surface at night and to depth during the day. For passive drifting, particles are moved by circulation only. Although evidence of vertical migration for echinoderms is very limited (Metaxas 2020; Doll et al. 2022), diel vertical migration has been widely observed for invertebrate larvae (Cohen and Forward 2009; Bandara et al. 2021) and is thus included in this study. With a 1 $km^2$ horizontal scale, the ocean circulation model does not reproduce circulation patterns that are smaller than 1 km, including nearshore circulation which has been hypothesized to retain larvae (Morgan et al. 2009, 2018; Hagerty et al. 2018; Yamhure et al. 2021). Thus, a relationship is derived from the number of times a particle passes through a source site to represent nearshore retention.

Using all possible combinations of the three larval life history parameters, 12 simulations are conducted over the 18-year modeling period for each of five ocean conditions, LDD, SZS, $T_L$, $T_S$ and Chl, determining how sensitive the ocean conditions are to variations in the larval life history parameters. All ocean conditions are found to be relatively insensitive to static versus

dynamic PLDs, but showed varying levels of sensitivity to both nearshore retention and larval behavior. LDD and SZS are found to be more sensitive to nearshore retention and larval behavior than Chl, $T_S$, and $T_L$. To determine which ocean conditions are the most likely drivers of larval recruitment in the SC Bight, all simulations of the ocean conditions are statistically compared to a larval recruitment index derived from larval recruitment data (Okamoto et al. 2020). $T_S$ is found to be the mostly likely driver to larval recruitment. LDD and SZS are found to potential drivers of larval recruitment if larvae are conducting DVM and influenced by nearshore retention, while $T_L$ and Chl are unlikely to be drivers of larval recruitment.

## 2.0 Methods

### *2.1 Biophysical Model*

To simulate larval transport, a 3D biophysical model consisting of two parts, an ocean circulation model (OCM) and a particle tracking model (PTM), was used. The OCM was a high-resolution Regional Ocean Modeling System (ROMS) applied to the SC Bight region (Dong and McWilliams 2007; Dong et al. 2009). The model domain, shown in Figure 1, contained the SC Bight and had 1 km horizontal resolution with 40 vertical levels. The model was thoroughly validated for mesoscale circulation (Dong et al. 2009) and has successfully reproduced upwelling events in the SC Bight (Dong et al. 2011; Simons and Catlett 2023) and eddy circulation in the Santa Barbara Channel (SBC, Simons et al. 2015). The temperature from the OCM was validated using temperature data from 26 stations in the SC Bight (see Supplementary Information (SI)). Six-hour averaged 3D flow fields and temperature solutions produced by the OCM from 1996-2013 were used for this study.

Larval transport was simulated using the 3D PTM driven by 3D flow fields produced by the OCM (Mitarai et al. 2009; Simons et al. 2013). For this project, the particle tracking was run in reverse time, which was possible since the ROMS flow fields and temperature solutions were stored offline. Reverse particle tracking was used to simulate the arrival of larvae at five recruitment sites in the SC Bight, Gaviota, Ellwood, Stearns, Anacapa, and Scripps, where larval recruitment has been recorded since 1993 (Figure 1, Schroeter et al. 2017; Okamoto et al. 2020). The PTM has been used extensively for larval transport in the SC Bight (Mitarai et al. 2009; Simons et al. 2016; Nishimoto et al. 2019; Page 2019), and validated against observational data from drifter experiments (Ohlmann and Mitarai 2010).

Particles were released from 45 horizontal locations evenly spaced every square kilometer around each recruitment site. This distribution of horizontal release points was selected to capture the mesoscale circulation in the area surrounding the recruitment sites. At each of the 45 horizontal release points, particles were released vertically every meter from 1 to 30 meters below the surface, the maximum depth where purple sea urchins are typically found. By evenly distributing particles over the water column, the particle distribution reflected average vertical flow conditions as recommended for robustness in biophysical models (Simons et al. 2013). Particles were released every 6 hours from the 1,350 vertical and horizontal locations at each recruitment site for 1996-2013 and tracked for 8 weeks. The tracking time of 8 weeks was selected because it is the maximum possible plankton larval duration under idealized conditions (Mustermann et al. 2025). The location and temperature of every particle trajectory was recorded every 6 hours. The particle release frequency was selected to meet the particle number criteria for model robustness (Simons et al. 2013).

The particles arriving at the recruitment sites must originate from a source site in the study area (Figure 1). Potential larval source sites in the SC Bight were identified by location of suitable spawning habitat for sea urchins. Suitable spawning habitat for sea urchins consists of rocky reef substrate located within kelp forests. Thus, the spatial distribution of larval source sites in the SC Bight was derived from satellite observations of giant kelp canopy (Bell et al. 2015). Using the mean distribution of giant kelp canopy from 1984-2022, suitable spawning habitat was found in 926 of the 1-km$^2$ model grid cells, which were designated as potential larval source sites (Figure 1).

To represent the recruitment season of purple sea urchins, which runs from March to June in the SC Bight (Okamoto et al. 2020), particles were released every 6 hours from March 1$^{st}$ to June 30$^{th}$ for every year of the modeling period (1996-2013) at the release locations for each recruitment site. Based on the particle release locations and frequency, a total of 12 million particles were released from each recruitment site over the 18-year modeling period.

To quantify the horizontal dispersal of particles, the 3D particle tracks were transformed into 2D particle density maps (PDMs). Using the three-dimensional particle tracks for each recruitment month and site, 2D monthly PDMs were produced by compiling the horizontal locations of all particle tracks from the particles released over the month into a single dataset and then summing the number of particle locations within each model grid cell of 1 km$^2$, creating a 2D particle density matrix the same size as the model grid. Example PDMs for the Gaviota and Scripps sites are shown in Figure 2(a-f).

*2.2 Larval life history parameters*

To accurately simulate the transport of purple sea urchin larvae in the SC Bight, larval life history parameters, which include planktonic larval duration (PLD), larval behavior, and nearshore retention, must be incorporated into the biophysical model. This section describes how each of these parameters was modeled.

PLD is represented in the PTM by the length of time particles are tracked. Two types of PLD were used for this study. The first PLD was 6 weeks, which was based on literature value and was termed “static PLD”. The second PLD was a temperature dependent PLD based on experimental studies (Mustermann et al. 2025), which was termed “dynamic PLD”. To model the static PLD, the particle tracking time was set to six weeks or 42 days. To calculate the dynamic PLD, the following two-step process was used. First, using all particle tracks for one recruitment site and month of the modeling period, the mean particle temperature was calculated for daily tracking times of 1 to 56 days. Second, the dynamic PLD was determined by the intersection of two lines of temperature versus PLD, one line from model results and the other line from the experimental data. This process was repeated for all recruitment sites and months of the 18-year modeling period, 1996-2013. The dynamic PLDs ranged from 26 to 56 days depending on the month, year, and recruitment site and are listed in Table S1.

Three types of larval behavior were simulated with the PTM, passive drifting and diel vertical migration to 20 m depth (DVM20) and 40 m depth (DVM40). To simulate passive drifting, particles were moved only by 3D currents. Diel vertical migration occurs when larvae migrate to the surface at night and to depth during the day (Cohen and Forward 2009). As the vertical movement or distribution of sea urchin larvae has not been studied in the SC Bight, depths of 20 m and 40 m were randomly selected to test this behavior. DVM20 and DVM40

were modeled by particles remaining at near-surface depths (~3 m) at night (18:00 hr to 06:00 hr) and at deeper depths of 20 m or 40 m during the day (06:00 hr to 18:00 hr). A basic random walk was used to vertically distribute the particles in a gaussian pattern around the set depths, near-surface, 20 m, and 40 m.

To quantify the effect of nearshore circulation on larval retention, two contrasting simulations, one without nearshore retention and one with nearshore retention, were produced. The simulation without nearshore retention assumed that particles travelled continuously from a source site to a recruitment site during their PLD and were not retained in a source site even if they passed through a source site during their PLD. As no information exists on the probability of larvae being retained along the shoreline, the simulations with nearshore retention assumed that the number of particles released during a recruitment month that passed through a source site at any time during their PLD was directly proportional to the probability of particles being retained within the source site. Thus, the simulations with nearshore retention contained all particle tracks that passed through a source site at any time during their PLD. If a particle track did not originate from a source site at the beginning of their PLD, the particle track was truncated at the first source site it entered, and the particle was then assumed to be retained within this source site for the portion of the PLD that it was not being transported to the recruitment site. Consequently, the PDMs without nearshore retention were created using only the particle tracks that start at a source site at the beginning of the their PLD, while the PDMs with nearshore retention were created using particle tracks that start a source site anytime during their PLD. This means that PDMs with nearshore retention include many

230 particle tracks that are shorter than the PLD and assume that these particles are retained within
231 the source site at the beginning of their PLD until they are transported to the recruitment site.

232 *2.3 Ocean conditions*

233 This section describes how the five ocean conditions, larval dispersal distance, source
234 zone strength, larval food supply, larval temperature, and temperature at the source sites, were
235 derived from particle tracking results. All ocean conditions are calculated on a monthly time-
236 scale for the modeling period of 1996-2013. Larval dispersal distance, source zone strength,
237 larval food supply, and larval temperature are calculated for the recruitment period of March to
238 June. Temperature at the source sites is calculated for the reproductive period of September to
239 November. For the larval life history parameters described in the previous section, only
240 nearshore retention changed the particle tracking times to less than the PLD. This change is
241 particle tracking times affected how source zone strength and larval temperature were
242 calculated with and without nearshore retention and is explained in this section.

243 <u>Larval Dispersal Distance (LDD)</u>

244 To compare larval dispersal between simulations, a monthly LDD for each recruitment
245 month and site was produced. The LDD was derived by calculating the distance between the
246 source site and recruitment site for each particle and then averaging this distance for all
247 particles tracked over the month. Thus, a monthly time-series of LDD for the recruitment period
248 was produced for each recruitment site in units of kilometers. To derive a mean LDD for the
249 entire 18-year study period, the LDD was averaged over all months and years of the study
250 period and is termed “mean LDD”.

251 <u>Source Zone Strength (SZS)</u>

Source site strength is defined as the relative probability that a larva spawned at a source site will arrive at a recruitment site (Mitarai et al. 2009; Watson et al. 2010). Source site strength for the recruitment period was derived by summing the number of particles that originated from or passed through a source site for one month of the modeling period at each recruitment site. Thus, the number of particles at each of the 926 source sites represents the relative probability or strength of the source sites. Without nearshore retention, source site strength was calculated using only the particles that originated at a source site at the beginning of the PLD and by counting each particle one time at its source site. With nearshore retention, source site strength was calculated using particles that originated at a source site anytime during the PLD and by counting the particle every time its track passed through a source site. Thus, the method for implementing nearshore retention resulted in particles being counted multiple times for different source sites. The source sites were geographically grouped into nine source zones (Figure 1). The nine source zones consisted of (1) the mainland of the SBC, (2) the north side of the North Channel Islands, (3) the south side of the North Channel Islands, (4-7) groups of contiguous source sites along the central and southern mainland of the SC Bight, (8) Catalina Island, and (9) three South Channel Islands. For each recruitment site and month, the percentage of particles in each zone was calculated, producing a monthly time-series of source zone strength (SZS) for each zone and recruitment site over the recruitment period.

Larval Food Availability (Chl)

To estimate food availability during larval transport, surface chlorophyll was used as a proxy for phytoplankton, which is what urchin larvae use for food. Surface chlorophyll for the SC Bight was calculated from satellite-derived 5-day composites of surface chlorophyll-a

concentrations (Kahru et al. 2012, 2015, https://spg-satdata.ucsd.edu) and was available from 1998 to 2013, 16 years of 18-year modeling period. As the satellite data is two-dimensional and does not represent the chlorophyll in the sub-surface, we recognize that this is a limitation of our analysis. However, surface chlorophyll has been shown to reflect the overall seasonal and interannual changes in chlorophyll in the SC Bight (Otero and Siegel 2004; Henderikx Freitas et al. 2017; Simons and Catlett 2023) and can provide some insight into the correlation between food availability and larval recruitment. In addition, satellite data was the only source of chlorophyll data that provided the spatial and temporal coverage needed to use with the particle tracking model results.

The 5-day composites of surface chlorophyll were averaged over each recruitment month of March-June to produce monthly surface chlorophyll of the SC Bight from 1998-2013. For each recruitment month and site, particle exposure to surface chlorophyll was calculated by first interpolating the model grid onto the monthly surface chlorophyll and then multiplying the surface chlorophyll in each model grid cell by the corresponding fraction of particles in the grid cell derived from the PDMs. Using this method, monthly time-series of larval exposure to chlorophyll (Chl) for each recruitment site was derived in units of mg $m^{-3}$.

Larval Temperature ($T_L$)

Larval temperature ($T_L$) represents the temperature that larvae are exposed to during their PLD. $T_L$ was derived from two sources of temperature produced by the OCM for the recruitment period. The first source was the particle temperature, which was recorded every 6 hours along the particle track. The second source was the temperature at the source sites, which was calculated every six hours at 5 m depth in the model grid cell where the source site

was located. A depth of 5 m was selected because it is the average depth of sea urchins in the SC Bight (Okamoto, D., personal observation). For simulations without nearshore retention, only particle temperature was used to calculate $T_L$ as particles were tracked for the entire duration of the PLD. In this case, $T_L$ was calculated by first averaging the particle temperature for each particle track, producing a mean particle temperature, and then averaging the mean particle temperatures for all the particles from one recruitment site and one month of the modeling period, producing a monthly time-series of $T_L$ for each recruitment site in units of °C for the recruitment period. For simulations with nearshore retention, both particle temperature and temperature at the source sites were used to calculate $T_L$ as many particles were retained at a source site for part of the PLD before being transported to a recruitment site. For the particles that were retained at a source site, the mean particle temperature was calculated by averaging the temperature at the source site for the time that the particle was retained there and the particle temperature for the time that the particle was tracked from the source site to the recruitment site. For the particles that were not retained at a source site, the mean particle temperature for particles was calculated the same way as the simulations without nearshore retention. Using both particles that were and were not retained at a source site, $T_L$ for simulations with nearshore retention was derived by averaging the mean particle temperatures from one recruitment site and one month of the modeling period, producing a monthly time-series of $T_L$ for each recruitment site in units of °C for the recruitment period.

Source Site Temperature ($T_S$)

The reproductive period for purple urchins in the SC Bight occurs from September to November. To assess the impact of temperature on adult urchins during the reproductive

period, temperature at the source sites ($T_S$), the location of the adult urchins, was needed. $T_S$ was calculated using the following four-step method. First, the monthly mean temperature at 5 m below the surface was calculated from the OCM at each of 926 source sites for the reproductive period from 1996-2013. Second, the monthly source site strength for the each of the 926 source sites was averaged over the recruitment period (March-June) for each year, producing yearly source site strength for each of the 18 years of the modeling period and each source site. Third, the yearly source site strength for each site was then divided by the sum of the yearly source site strength for all source sites, producing a fraction for each source site and year. As reproduction occurs prior to recruitment, the $T_S$ during the reproductive period was calculated from the source site strength for the following year and thus, limited to a 17-year modeling period of 1996-2012. Fourth, using the fractions derived from source site strength and temperature at the source sites, a weighted mean temperature or $T_S$ was calculated for each recruitment site and month of the reproductive period, producing a 17-year time-series of monthly $T_S$ for each recruitment site in units of °C.

*2.5 Sensitivity study of larval life history parameters*

Sensitivity of the five ocean conditions, LDD, SZS, Chl, $T_L$, and $T_S$ to variations in three larval life history parameters of PLD, larval behavior, and nearshore retention was tested. PLD had two options, static and dynamic. Behavior had three options, passive drifting, DVM20, and DVM40. Nearshore retention had two options, with retention and without retention. For each ocean condition, 12 simulations were created using all possible combinations of the three parameters and are listed in Table 1. Simulation 1 with passive drifting behavior, no nearshore

retention, and a static PLD was designated as the baseline simulation as it represents how larval transport is simulated for many other biophysical modeling studies (Swearer et al 2019).

| Simulation Number | Larval Life History Parameters | | |
|---|---|---|---|
| | Larval Behavior | Nearshore Retention | PLD |
| 1 | Passive Drifting | No | Static |
| 2 | Passive Drifting | No | Dynamic |
| 3 | Passive Drifting | Yes | Static |
| 4 | Passive Drifting | Yes | Dynamic |
| 5 | DVM20 | No | Static |
| 6 | DVM20 | No | Dynamic |
| 7 | DVM20 | Yes | Static |
| 8 | DVM20 | Yes | Dynamic |
| 9 | DVM40 | No | Static |
| 10 | DVM40 | No | Dynamic |
| 11 | DVM40 | Yes | Static |
| 12 | DVM40 | Yes | Dynamic |

Table 1: Simulations created for each of the five ocean conditions, LDD, SZS, Chl, $T_L$, and $T_S$, with three larval life history parameters of larval behavior, nearshore retention, and PLD.

For each ocean condition, simulations were compared using two statical measurements, root-mean-square deviation (RMSD) and Pearson's correlation coefficient (*r*). The RMSD was used to assess the absolute magnitude of deviation between the simulations. The *r* was used to assess the linear correlation between the simulations. To calculate RMSD and *r* for two simulations, the ocean conditions must be in the form of a 1D time-series, which is the case for LDD, $T_L$, Chl, and $T_S$. However, the SZS has 9 1D time-series, with each time-series corresponding to one zone. In order to calculate RMSD and *r* for two SZS simulations, the 9 SZS time-series for

each simulation were arranged into a 2D matrix with zone versus time and then linearized into a 1D vector.

To test each parameter, RMSD and *r* were calculated for two simulations where one parameter varied while the other two parameters were held constant. The two simulations are termed a 'simulation pair'. To test the sensitivity of an ocean condition to PLD, the RMSD and *r* was calculated for 6 simulations pairs (simulations 1 and 2, simulations 3 and 4, simulations 5 and 6, simulations 7 and 8, simulations 9 and 10, simulations 11 and 12), where one simulation had a static PLD and the other had a dynamic PLD while the choice of larval behavior and nearshore retention were the same in each pair. With two options, nearshore retention was tested with six simulation pairs (simulations 1 and 3, simulations 2 and 4, simulations 5 and 7, simulations 6 and 8, simulations 9 and 11, simulations 10 and 12). Larval behavior with three options was tested with 12 simulations pairs (simulations 1 and 5, simulations 2 and 6, simulations 3 and 7, simulations 4 and 8, simulations 1 and 9, simulations 2 and 10, simulations 3 and 11, simulations 4 and 12, simulations 5 and 9, simulations 6 and 10, simulations 7 and 11, simulations 8 and 12).

*2.5 Correlation of ocean conditions to larval recruitment index*

To determine which ocean conditions were most likely to be driving larval recruitment in the SC Bight, the ocean conditions were compared to an annual larval recruitment index that was derived from larval recruitment data. Recruitment indexes in the form of standardized larval settlement anomaly were available for the 5 recruitment sites including an additional site, Ocean Beach, which was located close to the Scripps recruitment site (Okamoto et al. 2020). A larval recruitment index was calculated for the northern SC Bight by averaging the indexes from

the four SBC recruitment sites, Gaviota, Ellwood, Stearns, and Anacapa, and for southern SC Bight by averaging the indexes from the recruitment sites for Scripps and Ocean Beach sites. Northern and southern SC Bight recruitment indexes were developed due to the synchronous patterns of recruitment at the northern versus the southern recruitment sites observed by Okamoto et al. (2020), indicating that forces driving recruitment are on a regional versus a local scale. As the recruitment indexes were on an annual time scale, the monthly time-series' of the ocean conditions were averaged over the recruitment period for LDD, SZS, Chl, and $T_L$, and over reproductive period for $T_S$ for each year to produce annual time-series'. The annual time-series of the ocean conditions were then compared to the northern recruitment index for the Gaviota, Ellwood, Stearns, and Anacapa recruitment sites and the southern recruitment index for the Scripps recruitment site by calculating *r* for the 12 simulations. LDD, $T_L$, Chl, and $T_S$ were in the form 1D time-series and could be used directly to calculate *r*, but SZS was a 2D time-series and had to be converted into a 1D time-series to compare to the 1D larval recruitment index. To do this, 1D SZS for each simulation and site was calculated by summing SZS over all possible combination of one to three zones. For the 9 zones, 129 combinations of 1 to 3 zones were used, producing 129 1D SZS time-series for each simulation and site. Then *r* was calculated between the 129 1D SZS time-series and the larval recruitment index, and the zones producing the largest positive and negative *r* values were used for the analysis. To indicate that any of the five ocean conditions may be driving recruitment, *r* would have to be of a similar high magnitude and sign across all recruitment sites for a single simulation.

## 3.0 Results

Our results are presented in two parts; first, the sensitivity of ocean conditions to the larval life history parameters and second, the correlation of ocean conditions to the larval recruitment index. The five ocean conditions fall into three categories: (1) ocean circulation represented by DD and SZS, (2) food supply represented by Chl and (3) temperature represented by $T_L$ and $T_S$. The larval life history parameters include PLD, nearshore retention, and behavior. PLD has two options, a static PLD of 42 days, and a dynamic PLD, which is as a function of temperature. Nearshore retention has two options, included or not included in the simulation. Behavior has three options, passive drifting, DVM with daytime depth of 20m (DVM20), and DVM with a daytime depth of 40m (DVM40). Using all possible combinations of these larval life history parameters, 12 particle tracking simulations, shown in Table 1, are produced for each of the ocean conditions and the recruitment sites over the 18-year modeling period of 1996-2013. Figures of the five ocean conditions for the 12 simulations are included in the SI.

### 3.1 Sensitivity of ocean conditions to larval life history parameters

<u>Larval Dispersal Distance</u>

Larval dispersal distance (LDD) represents the mean distance that the larvae have traveled from the source sites to the recruitment sites and reflects changes in circulation. For the baseline simulation of passive drifting behavior, a static PLD, and no nearshore retention, LDD is shown in Figure 3(a) for the recruitment period of March-June for the five recruitment sites. For the baseline simulation, LDD is extremely variable with each recruitment site ranging an order of magnitude over the modeling period. Baseline LDD for the modeling period

averages 79.5 km ± 51.6 km (mean±1 standard deviation) for Gaviota, 84.8 km ± 39.6 km for Ellwood, 99.7 km ± 30.8 km for Stearns, 71.1 km ± 25.3 km for Anacapa, and 88.4 km ± 47.8 km for Scripps. Baseline LDD is similar between the SBC sites of Gaviota, Ellwood, Sterns, and Anacapa, with RMSD from 24.5 to 30.7 km and *r* from 0.73 to 0.89, and distinctly different between the SBC sites and Scripps with RMSD from 73.0 to 94.2 km and *r* from -0.41 to -0.79.

To examine the sensitivity of LDD to PLD, the six simulations pairs with static versus dynamic PLD are compared and show very strong agreement for all recruitment sites. For all recruitment sites, RMSD ranges 1.8 -16.9 km, and *r* ranges from 0.95-0.99. These results suggest that LDD is mostly insensitive to changes in PLD.

For nearshore retention, the sensitivity testing of LDD for all recruitment sites shows a moderately strong linear correlation between all simulation pairs with and without nearshore retention for all sites, resulting in a *r* ranging from 0.73-0.96 with a mean of 0.88, but displays a large range of agreement in magnitude among the simulation pairs. For the SBC sites of Gaviota, Ellwood, Stearns, and Anacapa, the weakest agreement for LDD is observed for the two passive drifting simulation pairs with Gaviota, Ellwood, and Stearns showing weaker agreement than Anacapa. The two simulation pairs with passive drifting have RMSD ranging from 33.5 - 44.1 km for Gaviota, Ellwood, and Stearns and from 19.2-19.8 km for Anacapa. By calculating the mean error for the passive drifting simulation pairs, LDD is observed to decrease by 28.2-34.6 km for Gaviota, Ellwood, and Stearns and by 14.0-14.5 km for Anacapa when nearshore retention is included in the simulation (Figure 3(a,b)). For SBC sites, stronger agreement is observed for the four simulation pairs with DVM20 or DVM40 than the two simulations pairs with passive drifting. The simulation pairs with DVM20 and DVM40 have RMSD ranging from 11.7-25.6 km

for Gaviota, Ellwood, and Stearns and 11.4-18.8 km for Anacapa. By calculating the mean error between DVM20 and DVM40 simulations pairs for the SBC sites, LDD is observed to decrease by 4.6-10.9 km when nearshore retention is included, which is smaller than the passive drifting pairs. For Scripps, LDD shows similar magnitudes of agreement for all six simulation pairs with RMSD ranging from 55.7 – 67.0 km. By calculating the mean error between simulations pairs for Scripps, the simulation pairs with passive drifting and DVM20 show a decrease of 44.9-54.0 km in LDD when nearshore retention is included, while simulations with DVM40 show an increase of 19.2-21.8 km in LDD when nearshore retention is included.

In summary for nearshore retention, LDD from passive drifting is more sensitive to nearshore retention than LDD from DVM for the SBC sites. Among the SBC sites, LDD for Gaviota, Ellwood, and Stearns is more sensitive to nearshore retention than Anacapa for both passive drifting and DVM. For Scripps, LDD from passive drifting and DVM appears to be similarly sensitive to nearshore retention and more sensitive to nearshore retention than the SBC sites. For all sites, both passive drifting and DVM simulations produce a smaller LDD when nearshore retention is present.

For larval behavior, a clear pattern is observed for the SBC mainland sites of Gaviota, Ellwood, and Stearns with the weakest agreement in LDD for the four simulation pairs comparing passive drifting behavior to DVM20 or DVM40 without nearshore retention, the second weakest agreement in LDD for the four simulation pairs comparing passive drifting behavior to DVM20 or DVM40 with nearshore retention, and the strongest agreement in LDD for the four simulation pairs comparing DVM20 to DVM40 with and without nearshore retention. For the SBC mainland sites, the four simulation pairs comparing passive drifting

behavior to DVM20 or DVM40 without nearshore retention have the largest RMSD ranging from 60.2-74.3 km and the four simulation pairs comparing passive drifting behavior to DVM20 or DVM40 with nearshore retention have smaller RMSD ranging from 27.9-42.9 km. For these eight simulation pairs, *r* ranges widely from 0.30 and 0.69 with a mean of 0.49, and the strength of correlation is not associated with a specific larval behavior. By calculating the mean error for these eight simulations pairs, LDD decreases from 17.8-54.6 km with a mean of 38.6 km when DVM is included in the simulation. For the SBC mainland sites, the four simulation pairs comparing DVM20 to DVM40 with and without nearshore retention have the smallest RMSD ranging from 14.8-32.4 km and highest *r* ranging from 0.71-0.91. The mean error between these four simulations pairs is close to zero, indicating neither a significant increase or decrease in LDD between DVM20 and DVM40.

For larval behavior, LDD for Anacapa shows similar agreement for all simulations pairs with RMSD ranging from 20.1-28.7 km and *r* ranging from 0.56-0.75. LDD for Anacapa also displays the strongest agreement for all recruitment sites. In addition, the mean error for all simulation pairs is small, ranging from -10 to 15.4 km with a mean of 2.9 km, indicating no consistent increase or decrease in LDD associated with a specific behavior. Of the five recruitment sites, the Scripps site shows a largest range of agreement for the simulation pairs. The four simulation pairs comparing passive drifting to DVM20 or DVM40 with nearshore retention have the weakest agreement with RMSD ranging from 115-150 km and *r* ranging from 0.29-0.42. The four simulation pairs comparing passive drifting to DVM20 or DVM40 without nearshore retention have stronger agreement with RMSD ranging from 55-79 km and *r* ranging from 0.49-0.63. The four simulation pairs comparing DVM20 to DVM40 with and without

nearshore retention have the strongest agreement with RMSD ranging from 27-40 km and *r* ranging from 0.79-0.88. The mean error for Scripps shows an increase in LDD of 20-120 km for all simulation pairs, which means that LDD is larger for simulations with DVM20 or DVM40 than passive drifting and for simulations with DVM40 than DVM20 whether or not nearshore retention is included.

In summary for larval behavior, very different patterns of sensitivity are observed between the SBC mainland sites, Anacapa, and Scripps. For the SBC mainland sites, LDD is shows the weakest agreement between the passive drifting and DVM simulations without nearshore retention. Also, for the SBC mainland sites, the DVM simulations produce smaller LDDs than the passive drifting simulations, and this difference in LDD is greater when nearshore retention is not present. For Anacapa, LDD shows similarly strong agreement for all simulation pairs. For Scripps, LDD shows the weakest agreement between the passive drifting and DVM simulations with nearshore retention. Also, for Scripps, the addition of DVM decreases LDD when compared to passive drifting, which is the opposite of the SBC mainland sites.

Larval Source Zone Strength

Larval source zone strength (SZS) is defined as the probability that larvae have originated from a specified zone and represents how ocean circulation drives spatial and temporal variation in SZS. The nine source zones are identified in the SC Bight (Figure 1). The units for SZS are the percentage of particles per zone, which is directly proportional to SZS. SZS for the baseline simulation of passive drifting, a static PLD, and no nearshore retention is shown for the recruitment period of March-June in Figure 4(a-e) for all recruitment sites. For each recruitment site, baseline SZS is extremely variable with no clear patterns in time over the recruitment

period or space over the 9 zones. Baseline SZS for Gaviota is similar to Ellwood, Stearns, and Anacapa with RMSD ranging from 5-9% and *r* ranging from 0.72-0.90, but is different from Scripps with a RMSD of 18% and a *r* of 0.02. For the baseline simulation, the maximum SZS per month for Gaviota averages 36%±18% and is primarily associated with Zones 1-3 and 8-9. For Scripps, the maximum SZS per month for averages 40%±20% standard deviation and is primarily associated with Zones 6-7.

The sensitivity testing of SZS to PLD shows strong agreement for all simulation pairs with a static versus a dynamic PLD for all recruitment sites. For all simulation pairs and recruitment sites, the RMSD ranges 1-9%, and the *r* ranges from 0.88-1.0. These results suggest that SZS is largely insensitivity to differences in PLD.

For nearshore retention, patterns of agreement between SZS simulation pairs are similar for the SBC mainland sites of Gaviota, Ellwood, and Stearns. SZS for the SBC mainland sites shows the weakest agreement for the two simulation pairs comparing passive drifting with and without nearshore retention for, producing RMSD ranging from 12-21% and *r* ranging from 0.21-0.44. As shown in Figure 2(g,h) for Gaviota, the addition of nearshore retention to the simulation with passive drifting results in the highest SZS occurring in the Zone 1, where the recruitment sites are located. For Zone 1, the mean SZS over the modeling period increases from 24% to 71% for Gaviota, 18% to 61% for Ellwood, and 11% to 58% for Stearns when nearshore retention is included in the passive drifting simulation. For the SBC mainland sites, SZS shows the strongest agreement for the four simulation pairs comparing DVM20 or DVM40 with and without nearshore retention, producing RMSD ranging from 12-15% and *r* ranging from 0.73-0.91. Similar to the passive drifting simulation with nearshore retention, DVM20 and

DVM40 simulations with and without nearshore retention for the SBC mainland sites show the highest SZS consistently occurring in the Zone 1, explaining the strong agreement between these simulation pairs. For the SBC mainland sites, the mean SZS over the modeling period for Zone 1 ranges from 65-94% for DVM simulations with and without nearshore retention.

For nearshore retention, SZS for Anacapa and Scripps display different patterns of agreement from each other and the SBC mainland sites. For Anacapa, SZS shows similar agreement in magnitude for all simulation pairs with a RMSD ranging from 11-14%. The SZS for Anacapa shows a weaker linear correlation for the two passive drifting simulation pairs of *r* from 0.43-0.44 than the four DVM20 and DVM40 simulation pairs of *r* from 0.73-0.81. The increase in *r* between the passive drifting and DVM simulation pairs is similar to, but not as large as, the SBC mainland sites. The difference in SZS for the passive drifting simulation pairs is due to the consistent increase in SZS for Zone 2, where Anacapa is located, when nearshore retention is present. For the passive drifting simulations, the mean SZS in Zone 2 for Anacapa increases from 13% to 41% when nearshore retention is added. However, adding nearshore retention to the DVM simulations does not change the SZS significantly for Anacapa. For the DVM simulations with and without nearshore retention, the highest SZS for Anacapa is located in Zones 1-3, the three zones closest to Anacapa, and only increases from 64% to 74% for these zones when nearshore retention is added. For Scripps, the magnitude and linear correlation of SZS is very similar for all simulations pairs with RMSD ranging from 18-20% and *r* ranging from 0.47-0.64. This suggests that the addition of nearshore retention changes the linear correlation and magnitude of SZS about the same amount for both passive drifting and DVM. For all simulations, the highest SZS for Scripps is located in Zones 6, 7, and 9, the three zones closest to

the Scripps site, which increases when nearshore retention is added to the simulation (Figure 2(j,k)). The addition of nearshore retention increases the mean SZS over the modeling period for Zones 6, 7, and 9 from 67% to 95% for the passive drifting simulations and from 55% to 87% for the DVM simulations.

In summary for nearshore retention, SZS shows different patterns of sensitivities depending on the recruitment site. For the SBC mainland sites, SZS shows the weakest agreement between the passive drifting simulation pairs, which is due to the increase in Zone 1, where the SBC mainland sites are located, when nearshore retention is present. For Anacapa, SZS shows similarly small differences in magnitude for both passive drifting and DVM simulation pairs, but a range of linear correlations. Based on *r*, SZS for Anacapa is most sensitive to the passive drifting simulation pairs as nearshore retention produces an increase in SZS in Zone 2, where Anacapa is located. For Scripps, SZS shows similarly weak agreement for all simulation pairs as the presence of nearshore retention for both passive drifting and DVM increases the SZS in Zones 6, 7 and 9, which are nearest to Scripps.

The sensitivity testing of SZS to behavior shows the weakest agreement for the four simulation pairs comparing passive drifting to DVM20 or DVM40 without nearshore retention for the SBC mainland sites of Gaviota, Ellwood, and Stearns, producing RMSD ranging from 22-26% and *r* ranging from 0.10-0.36. For the SBC mainland sites, the passive drifting simulations without nearshore retention produce similarly low levels of SZS across all zones (Figure 2(g)), while the DVM20 or DVM40 simulations without nearshore retention produce the highest SZS in Zone 1, the zone where the recruitment site is located (Figure 2(i)). For Zone 1, the mean SZS over the modeling period increases from 19% to 63-71% for Gaviota, 15% to 60-66% for

572 Ellwood, and 11% to 59-62% for Stearns for the passive drifting versus the DVM simulations
573 without nearshore retention. The sensitivity testing of SZS displays the strongest agreement
574 between the eight simulation pairs comparing DVM20 to DVM40 with and without nearshore
575 retention and passive drifting to DVM20 or DVM40 with nearshore retention for the SBC
576 mainland sites, producing a RMSD ranging from 4-13% and a *r* ranging from 0.90-99. For the
577 SBC mainland sites, the mean SZS in Zone 1 over the modeling period is greater than 60% for all
578 eight simulations.

579 For Anacapa, testing the sensitivity of SZS to behavior shows the strongest agreement
580 for the four simulations pairs comparing DVM20 to DVM40, producing RMSD ranging from 8-
581 12% and *r* ranging from 0.80-0.88. For Anacapa, DVM20 and DVM40 simulations with and
582 without retention produce a pattern where the highest total SZS is spread over Zones 1 and 3,
583 which the two zones nearest the Zone 2 where the site is located. For Anacapa, the mean SZS
584 for Zones 1 and 3 over the modeling period ranges from 55-60% for the DVM20 and DVM40
585 simulations. SZS for Anacapa shows similarly weaker agreement for the eight simulations pairs
586 comparing passive drifting to DVM20 or DVM40, producing RMSD ranging from 14-18% and *r*
587 ranging from 0.35-0.60. For the passive drifting simulations, the mean SZS for Zones 1 and 3
588 over the modeling period is lower than the DVM20 and DVM40 simulations, ranging from 28-
589 29%.

590 For Scripps, the sensitivity testing of SZS shows the weakest agreement for the four
591 simulations pairs comparing passive drifting to DVM20 or DVM40 without nearshore retention,
592 producing RMSD ranging from 16-18% and *r* ranging from 0.43-0.50. SZS shows stronger
593 agreement of similar magnitude for the six simulations pairs comparing passive drifting to

DVM20 or DVM40 with nearshore retention and DVM20 to DVM40 without nearshore retention, producing RMSD ranging from 11-13% and *r* ranging from 0.78-0.90. SZS shows the strongest agreement for the two simulations pairs comparing DVM20 to DVM40 with nearshore retention, producing RMSD ranging from 4-5% and *r* ranging from 0.97-0.98. For Scripps, the passive drifting and DVM simulations without nearshore retention do not produce a pattern with high SZS occurring in specific zones, while the passive drifting and DVM simulations with nearshore retention produce a pattern with the highest total SZS occurring in Zones 6 and 7, which are nearest the Scripps site. For example, the highest mean SZS over the modeling period is 31% in Zone 7 for the passive drifting simulation without nearshore retention and 22% in Zone 6 for the DVM20 simulation without nearshore retention. In contrast, both the passive drifting and DVM20 simulations with nearshore retention produce a total SZS of 95% and 88% for Zones 6 and 7 respectively.

In summary for larval behavior, SZS displays a range of sensitivities as a function of recruitment site. For the SBC mainland sites, SZS shows the weakest agreement for the passive drifting and DVM simulation pairs without nearshore retention, which is driven by DVM increasing SZS in Zone 1, where the sites are located. For the SBC mainland sites, the remaining simulation pairs had similarly strong agreement due to both nearshore retention and DVM increasing SZS in Zone 1. For Anacapa, SZS shows the weakest agreement for the passive drifting and DVM simulations pairs with and without nearshore retention, which is driven by an increase in SZS for Zones 1 and 3, adjacent to the Zone where Anacapa is located. SZS for Scripps shows the weakest agreement for the passive drifting and DVM simulation pairs without nearshore retention, which is driven by no consistent pattern of the highest SZS occurring in specific zones.

Larval Food Availability

Larval food is represented by surface chlorophyll (Chl), which is available from 1998-2013, 16 years of the modeling period. For the five recruitment sites, Chl for the baseline simulation of passive drifting behavior, a static PLD, and no nearshore retention, is shown in Figure 3(c) for the recruitment period of March-June. Baseline Chl is most similar between the Gaviota site and the Ellwood and Stearns sites with a RMSD of 0.70 mg $m^{-3}$ and 0.75 mg $m^{-3}$ and a *r* of 0.94 and 0.90 respectively and least similar between the Gaviota site and the Anacapa and Scripps sites with a RMSD of 1.24 mg $m^{-3}$ and 1.57 mg $m^{-3}$ and a *r* of 0.88 and 0.74 respectively. Averaged over the modeling period, baseline mean Chl is 2.95 mg $m^{-3}$, 2.65 mg $m^{-3}$, 2.74 mg $m^{-3}$, 2.06 mg $m^{-3}$, and 1.84 mg $m^{-3}$ for Gaviota, Ellwood, Stearns, Anacapa, and Scripps respectively. The baseline mean Chl is similar between the SBC mainland sites, Gaviota, Ellwood, and Stearns, and shows a decrease from Gaviota to Anacapa to Scripps, reflecting the north-south gradient of Chl in the SC Bight (Figure 5(a)).

The sensitivity testing of Chl to PLD shows strong agreement between the simulation pairs with a static PLD versus a dynamic PLD. For the six simulation pairs tested, the RMSD ranges 0.10-0.37 mg $m^{-3}$, and the *r* ranges from 0.98-1.0. These results suggest that Chl is relatively insensitive to PLD for all recruitment sites.

For nearshore retention, the sensitivity testing of Chl for all recruitment sites shows a strong linear correlation between all simulation pairs with and without nearshore retention, resulting in an *r* ranging from 0.91-1.0, but displays a range of agreement in magnitude among the simulation pairs. For all recruitment sites, Chl shows a weaker agreement in magnitude for the two passive drifting simulations pairs with RMSD ranging 0.49-0.80 mg $m^{-3}$ with a mean of

0.61 mg $m^{-3}$ (Figure 3(c,d)) than the four DVM20 and DVM40 simulation pairs with RMSD ranging 0.29-0.66 mg $m^{-3}$ with a mean of 0.43 mg $m^{-3}$. The passive drifting simulations with nearshore retention have a higher mean Chl of 0.31-0.68 mg $m^{-3}$ over the modeling period than the passive drifting simulations without nearshore retention. In contrast, mean Chl is similar in magnitude for DVM simulations with and without nearshore retention. These results suggest that Chl for all recruitment sites is more sensitive to the addition of nearshore retention to passive drifting behavior than to DVM20 or DVM40 behavior.

For larval behavior, Chl shows strong linear correlations for the 12 simulation pairs for all recruitment sites with *r* ranging from 0.80 – 0.99, but a range of differences in magnitude. For the SBC sites of Gaviota, Ellwood, Stearns, and Anacapa, Chl shows the weakest agreement for the eight simulation pairs comparing passive drifting to DVM20 or DVM40 with a RMSD ranging from 0.67-1.62 mg $m^{-3}$. For these eight simulation pairs, the mean Chl for the DVM simulations is greater by an average of 0.51 mg $m^{-3}$ than the mean Chl for the passive drifting simulations. For the SBC sites, Chl shows the strongest agreement for the four simulation pairs comparing DVM20 and DVM40 with a RMSD ranging from 0.04-0.38 mg $m^{-3}$ and very similar mean Chl with an average difference of 0.02 mg $m^{-3}$. For Scripps, Chl shows a range of agreement for the 12 simulations pairs, but the magnitude of agreement is not correlated with larval behaviors. For Scripps, Chl shows a RMSD ranging from 0.27-0.74 mg $m^{-3}$. Thus, for larval behavior, Chl for the SBC sites shows more sensitivity between passive drifting and DVM20 or DVM40 than between DVM20 and DVM40. Chl for Scripps is inconsistently sensitive to specific larval behaviors.

<u>Larval Temperature</u>

Larval temperature ($T_L$) is defined as the temperature that larvae are exposed to during the PLD. $T_L$ for the baseline simulation of passive drifting behavior, a static PLD, and no nearshore retention is shown in Figure 3(e) for the recruitment period of March-June for the five recruitment sites. For the baseline simulation, $T_L$ for all months and recruitment sites is below 16°C and ranges from 9.7-15.6°C. For all recruitment sites, the yearly change in baseline $T_L$ over the recruitment period averages 1.5°C with a maximum of 2.8°C and does not show a consistent pattern of warming or cooling. Baseline $T_L$ is very similar between mainland SBC sites of Gaviota, Ellwood, and Stearns. Comparing baseline $T_L$ at Gaviota to Ellwood and Stearns, RMSD and *r* range from 0.28-0.45°C and 0.92-0.96 respectively. Greater differences in baseline $T_L$ are observed between Gaviota and Anacapa with a RMSD of 0.75°C and a *r* of 0.86 and between Gaviota and Scripps with a RMSD of 1.4°C and a *r* of 0.59. Averaging over the modeling period, baseline mean $T_L$ is 12.4°C, 12.9°C, and 13.5°C for Gaviota, Anacapa, and Scripps respectively, reflecting the north-south temperature gradient in the SC Bight (Figure 5(b)).

The sensitivity testing of $T_L$ to PLD shows strong agreement between the six simulation pairs comparing static versus dynamic PLD. For the six simulation pairs and all recruitment sites, the RMSD ranges 0.13-0.36°C with a mean of 0.17°C, and the *r* ranges from 0.96-0.99 with a mean of 0.99. These results imply that $T_L$ is largely insensitive to changes in PLD.

The sensitivity testing of $T_L$ to nearshore retention shows strong linear correlations for all simulation pairs and recruitment sites with *r* ranging from 0.83-0.98 with a mean of 0.93. However, differences in magnitude of $T_L$ are observed with the weakest agreement for the simulation pairs with passive drifting (Figure 3(e,f)and the strongest agreement for the simulation pairs with DVM20 or DVM40 for all recruitment sites. $T_L$ for the two simulation pairs

with passive drifting have a RMSD ranging from 0.54-0.80°C with a mean of 0.63°C for the SBC sites of Gaviota, Ellwood, Stearns, and Anacapa and a RMSD ranging from 0.87-1.0°C with a mean of 0.93°C for Scripps. In contrast, the four simulation pairs with DVM20 or DVM40 have a RMSD ranging from 0.21-0.44°C with a mean of 0.30°C for the SBC sites and a RMSD ranging from 0.55-0.82°C with a mean of 0.65°C for Scripps. Thus, $T_L$ for all recruitment sites is more sensitive to the addition of nearshore retention to passive drifting simulations than to DVM20 or DVM40 simulations.

The sensitivity testing of $T_L$ to behavior shows strong linear correlations for all simulation pairs and recruitment sites with *r* ranging from 0.85-0.99 with a mean of 0.93, but a range of agreement in magnitude. For the SBC mainland sites, $T_L$ shows the weakest agreement for the four simulation pairs comparing passive drifting to DVM20 or DVM40 without nearshore retention, which have a RMSD ranging from 0.44-0.91°C with a mean of 0.64°C, and the strongest agreement for the four simulation pairs comparing DVM20 to DVM40 with or without nearshore retention, which had a RMSD ranging from 0.23-0.35°C with a mean of 0.29°C. For Anacapa and Scripps, $T_L$ has the weakest agreement for the two simulation pairs comparing passive drifting to DVM20 without nearshore retention, which had a RMSD ranging from 0.49-0.54°C and 0.71-0.80°C respectively, but shows similarly stronger agreement for the ten other simulations pairs, which had a RMSD ranging from 0.24-0.49°C with a mean of 0.35°C for Anacapa and from 0.34-0.53°C with a mean of 0.42°C for Scripps. Thus, $T_L$ for the SBC mainland sites shows weaker agreement between DVM and passive drifting simulations when nearshore retention is absent than when nearshore retention is present and strong agreement between DVM20 and DVM40 regardless if nearshore retention is present. For Anacapa and Scripps, $T_L$

shows the weakest agreement between passive drifting and DVM20 simulations without nearshore retention.

Source Site Temperature

Source site temperature ($T_S$) is defined as the temperature that adult urchins at the source sites are exposed to during the reproductive period of September to November. Since the reproductive period occurs in the fall while spawning and recruitment occurs in the following spring, the modeling period for $T_S$ is limited to 17 years from 1996-2012. $T_S$ for the baseline simulation of passive drifting, a static PLD, and no nearshore retention is shown in Figure 3(g) for all five recruitment sites. For all months and recruitment sites, $T_S$ for the baseline simulation is above 14°C and ranges from 14.2-20.5°C. For all years except 1998, the baseline $T_S$ decreases over the reproductive period with the change in $T_S$ ranging from 0.5°C to 4°C and averaging 2.4°C. When baseline $T_S$ at Gaviota is compared to the other recruitment sites, $T_S$ is found to have a strong linear correlation for all sites with *r* ranging from 0.97 to 1.0. Baseline $T_S$ at Gaviota is similar in magnitude to the three the SBC sites of Ellwood, Stearns, and Anacapa with RMSD ranging from 0.14-0.25°C. The largest difference in magnitude of baseline $T_S$ is between Gaviota and Scripps with a RMSD of 0.49°C, reflecting the north-south temperature gradient in the SC Bight (Figure 5(c)).

The sensitivity testing of $T_S$ to PLD shows strong agreement for simulation pairs with static and dynamic PLD for all recruitment sites. For the six simulation pairs tested for PLD, the RMSD ranges from 0.02-0.22°C with a mean of 0.11°C, and the *r* ranges from 0.99-1.00 with a mean of 1.00. These results suggest that $T_S$ is largely insensitive to PLD.

Testing the sensitivity of $T_S$ to nearshore retention shows strong linear correlations for all simulation pairs and recruitment sites with *r* ranging from 0.91-1.00 with a mean of 0.97, but a range of differences in magnitude. For the SBC mainland sites of Gaviota, Ellwood, and Stearns, the sensitivity testing of $T_S$ to nearshore retention shows the weakest agreement in magnitude for the two passive drifting simulation pairs, which produce RMSD ranging from 0.68-1.1°C with a mean of 0.85°C, and the strongest agreement in magnitude for the four DVM20 and DVM40 simulation pairs, which produce RMSD ranging from 0.19-0.45°C with a mean of 0.29°C. For Anacapa, the sensitivity testing of $T_S$ to nearshore retention shows a similar but less pronounced pattern as the SBC mainland sites with the two passive drifting simulation pairs producing RMSD ranging from 0.43-0.45°C and the four DVM20 and DVM40 simulation pairs producing RMSD ranging from 0.17-0.27°. For Scripps, sensitivity testing of $T_S$ to nearshore retention does not show changes in magnitude that correlate with behavior and produces RMSD ranging from 0.38-0.52°C for all simulation pairs. Thus, $T_S$ for the SBC mainland sites and Anacapa is more sensitive to nearshore retention for passive drifting than DVM. For Scripps, $T_S$ shows similar levels of sensitivity to nearshore retention for passive drifting and DVM.

Testing the sensitivity of $T_S$ to behavior shows strong linear correlations for all simulation pairs and recruitment sites with *r* ranging from 0.86-0.99 with a mean of 0.97. Sensitivity testing of $T_S$ to behavior shows the weakest agreement for the four simulation pairs comparing passive drifting to DVM20 or DVM40 without nearshore retention for the SBC mainland sites, producing RMSD ranging from 0.97-1.2°C with a mean of 1.1°C. In comparison, $T_S$ for the SBC mainland sites show the strongest agreement for the eight simulation pairs comparing DVM20 to DVM40 with and without nearshore retention and passive drifting to DVM20 or DVM40 with nearshore

retention, producing RMSD ranging from 0.07-0.47 °C and a mean of 0.28 °C. For Scripps and Anacapa, $T_S$ follows the same pattern as the SBC mainland sites, but shows overall stronger agreement. $T_S$ for the four simulation pairs comparing passive drifting to DVM20 or DVM40 without nearshore retention produce RMSD ranging from 0.60-0.67°C with a mean of 0.63°C for Anacapa and from 0.28-0.33°C with a mean of 0.31°C for Scripps. $T_S$ for the eight simulation pairs comparing DVM20 to DVM40 with and without nearshore retention and passive drifting to DVM20 or DVM40 with nearshore retention produce smaller RMSD ranging from 0.13-0.35°C and a mean of 0.28°C for Anacapa and from 0.05-0.22°C and a mean of 0.15°C for Scripps. For all sites, $T_S$ shows the weakest agreement for passive drifting and DVM simulation pairs when nearshore retention is not present and the strongest agreement for passive drifting and DVM simulations pairs when nearshore retention is present and for DVM20 and DVM40 simulation pairs with and without nearshore retention. $T_S$ for the SBC mainland sites displays higher levels of sensitivity than for Anacapa and Scripps.

*3.2 Comparison of ocean conditions to larval recruitment index*

To determine the influence of the ocean conditions on larval recruitment, the 12 simulations for each ocean condition are linearly correlated to a larval recruitment index for all recruitment sites. A meaningful linear correlation between an ocean condition and the larval recruitment index should have strong agreement or high values of *r*. A northern SC Bight recruitment index is used for the Gaviota, Ellwood, Stearns, and Anacapa sites, which has five poor recruitment years of 1998 and 2004-2007 and 13 average or above average recruitment years. A southern SC Bight recruitment index is used for the Scripps site, which has five average and above-average recruitment years of 1996 and 1999-2002 and 13 poor recruitment years.

When $T_L$ and Chl are compared to the larval recruitment index for all simulations and recruitment sites, only a weak and inconsistent linear correlation is found. For $T_L$, *r* ranges from -0.35 to 0.29 with a mean of -0.13 for all simulations and recruitment sites. For Chl, *r* ranges from -0.52 to 0.05 with a mean of -0.13 for all simulations and recruitment sites. These results suggest that that larval temperature and larval food supply are not likely drivers of larval recruitment of purple sea urchins in the SC Bight.

The strength of correlation between LDD simulations and the larval recruitment index varies as a function of larval behavior, nearshore retention, and recruitment site. For the SBC sites of Gaviota, Ellwood, Stearns, and Anacapa, the strength of correlation is related to the larval behavior. For passive drifting simulations, LDD for SBC sites has the weakest correlations with *r* ranging from -0.23 to 0.24 and averaging -0.04. For DVM20 simulations, LDD for Gaviota, Ellwood, and Stearns has stronger correlations than the passive drifting simulations with *r* ranging from -0.15 to -0.28 and averaging -0.23, but LDD for Anacapa has similarly weak correlations as the passive drifting simulations with *r* ranging from -0.07 to 0.0 and averaging -0.02. For DVM40 simulations, LDD has the highest correlations with *r* ranging from -0.22 to -0.54 and averaging -0.33 for Gaviota, Ellwood and Stearns and with *r* ranging from -0.18 to -0.30 and averaging -0.25 for Anacapa. For Scripps, LDD has similarly strong correlations for all simulations with *r* ranging from -0.48 to -0.73 and a mean of -0.61. The negative *r* indicates that LDD is inversely proportional to the larval recruitment index, meaning that the shorter LDD is correlated with higher recruitment and vice versa.

To display the strongest linear correlation between LDD and larval recruitment index, Figure 6(a,b) shows plots of LDD versus the larval recruitment index for the simulation with

DVM40, nearshore retention, and a static PLD for Gaviota and Scripps. Gaviota and Scripps are shown because they are recruitment sites that are farthest apart and represent the northern versus southern ocean conditions in the SC Bight. Gaviota and Scripps have a similar *r* of -0.53 and -0.64 respectively for this simulation, but the LDD is much larger and more variable for Scripps with an average LDD of 151 km $\pm$ 93 km (mean $\pm$ 1 standard deviation) than for Gaviota with an average LDD of 19 km $\pm$ 6 km. For Gaviota shown in Figure 6(a), the four poor recruitment years (2004-2007) have larger LDDs of 28.4-31.1 km than the thirteen average to above-average recruitment years (1996-1997, 1999-2003, 2008-2013), which have LDDs of 12.7-17.8 km. Only 1998 deviates significantly from correlation with the smallest LDD of 10.3 km and a very low recruitment index. The linear regression model for Gaviota, shown in Figure 6(a), is *RI* = -0.105*LDD+2.077 where *RI* is the larval recruitment index and LDD is in km. For Scripps shown in Figure 6(b), all five average to above-average recruitment years (1996, 1999-2002) correlate with small LDDs of 33-71 km. The ten show poor recruitment years (2004-2013) have very large LDDs ranging from 210-248 km. Three years (1997, 1998, 2003) significantly deviate from correlation with small LDDs of 71-85 km and poor recruitment. The linear regression model for Scripps, shown in Figure 6(b), is *RI* = -0.006*LDD+0.8641 where *RI* is the larval recruitment index and LDD is in km.

For all sites and simulations, SZS displays a positive *r* ranging from 0.27-0.76 and averaging 0.45 and negative *r* ranging from -0.31 to -0.79 and averaging -0.52. The zones optimized to produce the highest positive and negative *r* values for all sites and simulations are show in Table S2. The simulations with DVM20 behavior, no nearshore retention, and a static or dynamic PLD had the highest positive and negative *r* values, ranging from 048 to 0.70 and from -

0.53 to -0.71. To display the linear correlation between SZS and the larval recruitment index, Figure 6(c-f) shows plots of SZS for positive and negative *r* values versus larval recruitment index for the simulation with DVM20, no nearshore retention, and a static PLD for Gaviota and Scripps.

For Gaviota, this simulation has a positive *r* value of 0.55 for Zones 1 and 3, which are located along the SBC mainland and the south coast of the Northern Channel Islands, and a negative *r* value of -0.58 for Zones 4, 8, and 9, which are located along the central SC Bight mainland and the Southern Channel Islands (Figure 1). As shown in Figure 6(c) for Gaviota, 81%±11% (mean ± 1 standard deviation) of the particles come from zones near the SBC, where the Gaviota site is located, in average and above-average recruitment years. In poor recruitment years, only 50%±19% of particles come from these zones near the SBC and instead come from the zones south of the SBC. One year, 1998, does not follow this pattern with very poor recruitment, but a high percentage of particles coming from the zones near the SBC. For Gaviota, the linear regression model shown in Figure 6(c) is $RI = 0.0348*SZS-2.5005$ where *RI* is the larval recruitment index and *SZS* is the SZS for positive *r* in percentage and in Figure 6(d) is $RI = -0.0406*SZS+0.8190$ where *RI* is the larval recruitment index and *SZS* is the SZS for negative *r* in percentage.

For Scripps, the simulation with DVM20, no nearshore retention, and a static or dynamic PLD has a positive *r* value of 0.70 for Zones 6 and 7, which are located along the southern SC Bight mainland (Figure 1). The Scripps site is located in Zone 7 and Zone 6 is directly north of Zone 7 along the mainland coast. The simulation with DVM20, no nearshore retention, and a static PLD for Scripps has a negative *r* value of -0.71 using Zones 4, 5, and 9, which are located in

along the central SC Bight mainland and the South Channel Islands (Figure 1). For Scripps, 80%±15 of particles come from zones on the southern SC Bight mainland, where the Scripps site is located, in average and above-average recruitment years. In a poor recruitment year, only 35%±15% of larvae come from these zones and instead come from the zones in central SC Bight mainland and the South Channel Islands. The linear regression model for Scripps, shown in Figure 6(e,f), is $RI = 0.0219*SZS-1.2055$ where $RI$ is the larval recruitment index and $SZS$ is the SZS for positive $r$ in percentage and $RI = -0.0463*SZS-0.9907$ where $RI$ is the larval recruitment index and $SZS$ is the SZS for negative $r$ in percentage.

Out of all the ocean conditions, $T_S$ shows the highest correlation with the larval recruitment index, producing a mean $r$ of -0.69 with a standard deviation of 0.08 for all sites and all simulations. The negative $r$ means that high $T_S$ produces to low recruitment and that low $T_S$ produces high recruitment. For the SBC mainland sites, $T_S$ simulations that have DVM and/or nearshore retention produce a higher correlation with $r$ ranging from -0.66 to -0.78 and averaging -0.74 than the $T_S$ simulations that have passive drifting without nearshore retention with $r$ ranging from -0.44 to -0.55. For Anacapa and Scripps, $T_S$ produces correlations with $r$ ranging from -0.56 to -0.80 and averaging -0.68 and where correlation strength is not connected to a larval behavior or nearshore retention.

To display the linear correlation between $T_S$ and larval recruitment index, Figure 6(g,h) shows plots of $T_S$ versus the larval recruitment index for the simulation with passive tracking, nearshore retention, and a static PLD for Gaviota and Scripps. Gaviota and Scripps have a similar $r$ of -0.73 and -0.72 for this simulation. For Gaviota, the 13 years with average to above-average recruitment (1996-1997, 1999-2003, 2008-2013) correlate with lower $T_S$ ranging from 14.9-

16.6°C and averaging 16.0°C. Three of the poor recruitment years, (1998, 2005, 2007) correlate with higher $T_S$ of 17.8-18.0°C, but the poor recruitment years of 2004 and 2006 deviate from the linear correlation with $T_S$ of 16.4°C and 16.5°C respectively. The linear regression model for Gaviota, show in 7(g), is $RI = -0.839*T_S+13.696$ where *RI* is the larval recruitment index and $T_S$ is in °C. For Scripps, the 13 poor recruitment years (1997, 2003-2013) have higher $T_S$, ranging from 17.6-19.9°C and averaging 18.2°C. The four years (1999-2002) with average to above-average recruitment have lower $T_S$ ranging from 15.9-17.6 °C and averaging 17.1°C. The linear regression model for Scripps, shown in Figure 7(h), is $RI = -0.587*T_S+10.294$ where *RI* is the larval recruitment index and $T_S$ is in °C.

## 4.0 Discussion

The goal of this study is to assess the impacts of changes in circulation, temperature, and food supply on larval recruitment of purple sea urchins. Changes in circulation are quantified using LDD and SZS, which are calculated directly from particle tracks. Temperature is quantified through $T_L$ and $T_S$, which are calculated from the OCM's temperature and particle tracks. Food supply is quantified using Chl, which is calculated from surface chlorophyll from satellite data and particle tracks. To accurately model larval recruitment, the larval life history of purple sea urchins must be accurately represented in the biophysical model. Although some aspects of the larval life history of purple sea urchins are known, such as the spawning and reproductive periods and potential source sites, uncertainty remains for three important aspects of larval life history, PLD, nearshore retention, and larval behavior. To address this uncertainty, sensitivity of the five ocean conditions to these three larval life history parameters is discussed in Section 4.1. Derived from the 12 simulations with all possible combinations of larval life history parameters,

each ocean condition is then compared to a larval recruitment index to identify the potential drivers of larval recruitment, which is discussed in Section 4.2.

*4.1 Sensitivity of ocean conditions to larval life history parameters*

PLD, the first larval life history parameter, shows very strong agreement between the simulation pairs with static and dynamic PLDs for all five ocean conditions. This result initially appears surprising as the static PLD at 42 days is significantly different from the dynamic PLD, which ranges from 26-57 days with a mean of 37 days (SI Table S1). However, Simons et al. (2013) found that particle dispersal in the SC Bight is much more sensitive to changes in particle tracking times or PLDs when PLDs are greater than ~20 days and concluded that the changes in particle dispersal patterns decrease with increasing PLD because the particles become more evenly mixed over increasingly larger areas. To determine if this may be true for this study, *r* is calculated between the PDMs with a PLD of 42 days and the PDMs with PLDs of 1-56 days for each month, simulation, and recruitment site, producing a total of 4,320 vectors of daily *r* from 1-56 days. As PDMs are 2D particle density matrices, the PDMs are vectorized for a grid cell to grid cell calculation of *r* following the methods in Simons et al. (2013). Figure 7 displays mean *r* $\pm$ 1 standard deviation versus PLD for all *r* vectors and shows that there is minimal difference between the PDMs with a 42-day PLD and PDMs with PLDs greater than ~25 days. As all ocean conditions are derived from the particle tracks, which are used to create the PDMs, this similarity between the PDM with a PLD of 42-days and PDMs with PLDs greater than ~25 days explains why the ocean conditions are relatively insensitive to the static PLD of 42 days versus the dynamic PLD of 26-57 days. Based on these results, the following discussion of sensitivity to

nearshore retention and larval behavior does not distinguish between the simulations with static PLD and dynamic PLD.

Three main trends are observed in the sensitivity testing that apply to both nearshore retention and larval behavior. The first trend is that the ocean conditions representing circulation, LDD and SZS, show much higher sensitivity than the ocean conditions representing food supply, Chl, and temperature, $T_L$, and $T_S$, for all simulations and recruitment sites. The second trend is that simulation pairs show similar levels of sensitivity for all ocean conditions for the SBC mainland sites, but not for the Anacapa and Scripps sites. The third trend is that two simulation pairs, one for nearshore retention and one for larval behavior, show the highest sensitivity for all ocean conditions. For nearshore retention, the simulations pair is the passive drifting simulation without nearshore retention versus the passive drifting simulation with nearshore retention. For larval behavior, the simulation pair is the passive drifting simulation without nearshore retention versus the DVM20 simulation without nearshore retention.

In order to compare the level of sensitivity between ocean conditions, which have different units, RMSD for each ocean condition is normalized by dividing the RMSD by the mean ocean condition for both simulations in the pair, producing a RMSD percentage for each simulation pair. RMSD percentage is calculated for the nearshore retention and larval behavior simulation pairs with the highest sensitivity and the five ocean conditions. SZS has the highest RMSD percent for all sites and both simulation pairs, ranging from 110-210% with a mean of 174%. LDD for all sites and both simulation pairs has the next highest RMSD percent, ranging from 30-110% with a mean of 68%. For all sites and both simulation pairs, $T_L$ and $T_S$ have the lowest RMSD percent by 1-2 order of magnitudes compared SZS, LDD, and Chl, ranging from 2-

7% with a mean of 5%. RMSD percent for Chl falls in the middle of the ocean conditions, ranging from 19-52% with a mean of 34%. In general, the larval behavior simulation pair has a higher RMSD percent than the nearshore retention simulation pair.

Our results suggest that these trends are driven by the difference in circulation, temperature, and surface chlorophyll in the northern versus the southern SC Bight. Figure 5(d) shows the mean velocity from the OCM over the top 50 m of the water column in the SC Bight for the recruitment period of March-June and modeling period. The top 50 m of the water column is selected because an average of ~70% of the particles with passive drifting remain the top 50 m of the water column during their PLD. Figure 5(a-c) displays the mean temperature from the OCM averaged over the top 50 m of the water column for the reproductive and recruitment periods and the mean chlorophyll from satellite data averaged over the recruitment period. As shown in Figure 5, the circulation, temperature, and surface chlorophyll for the regions near each recruitment site are described below.

In the northern SC Bight, the mean circulation in the SBC, where the SBC mainland sites are located, is dominated by a cyclonic eddy, which has the strongest mean velocities in the SC Bight up to 21 cm $s^{-1}$ and penetrates throughout the top 100 m of the water column (Dong et al. 2009; Brokaw et al. 2024). The strong eddy circulation creates a region of high residence times and particle accumulation in the SBC (Simons et al. 2015; Simons and Catlett 2023). The SBC is the coldest region in the SC Bight with mean temperatures 4-5°C lower than the region east of the Scripps site (Figure 5(b,c)). The mean temperature immediately surrounding the SBC are ~1.5°C higher than the mean temperature within the SBC. Driven by spring upwelling and high residence times in the SBC (Simons and Catlett 2023; Brokaw et al. 2024), the mean surface

chlorophyll in the SBC is the highest in SC Bight with a maximum of 2.7 mg $m^{-3}$ and drops to low levels of 0.1 - 1 mg $m^{-3}$ outside of the SBC.

Located on Anacapa Island on the edge of the SBC, the Anacapa site is surrounded by the weakest mean velocities, ~3 cm $s^{-1}$, of the five recruitment sites and sits at the junction between flows entering the SBC and the large cyclonic eddy in the central SC Bight, which both influence transport in the region of the Anacapa site. The Anacapa site is located in the transition zone between the SBC and the central and southern SC Bight, where strong gradients in mean temperature and surface chlorophyll are present.

In the southern SC Bight, the circulation near the Scripps site shows southward flow along the coastline with mean velocities up to 10 cm $s^{-1}$ and which decreases an order of magnitude to the north and east. Unlike the SBC which has consistent mean circulation with depth, mean circulation along the southern coastline varies with depth, displaying stronger southward flows in the top 50 m of the water column and weaker northward flows from 50-100 m depth (Dong et al. 2009). Defined by an open coastline with a narrow shelf, circulation in the region near the Scripps site produces shorter residence times and greater offshore dispersal than the SBC (Dong et al. 2012). Except for ~5 km adjacent to the coastline, the southern SC Bight displays smaller north-south mean temperature gradients of 0.1-0.2°C per 10 km than the area surrounding the SBC of 0.3-0.4°C per 10 km. The mean surface chlorophyll throughout the southern SC Bight is very low from 0.1-1 mg $m^{-3}$.

To understand why the ocean conditions show different levels of sensitivity, we evaluate the connection between circulation and particle dispersal. To quantify particle dispersal, mean PDMs representing the three simulations used in the nearshore retention and larval behavior

simulation pairs with the highest sensitivity are displayed in Figure 2 for the Gaviota and Scripps sites. The three simulations are (1) passive drifting without nearshore retention (Figure 2(a,d)), (2) passive drifting with nearshore retention (Figure 2(b,e)), and (3) DVM20 without nearshore retention (Figure 2(c,f)). All simulations shown have a static PLD. The Gaviota and Scripps sites are selected because they reflect the different circulation in the northern SBC versus the southern SC Bight.

When nearshore retention is included in a simulation, the number particles coming from source sites near the recruitment site automatically increases as simulations with nearshore retention includes all particle tracks from a source site to a recruitment site that are at or below the PLD, e.g. PLDs less than or equal to 42 days. In comparison, simulations without nearshore retention only include particle tracks from a source site to a recruitment site at the exact PLD, e.g. PLDs equal 42 days. The increase in particle concentrations near the Goleta and Scripps sites when nearshore retention is applied to the passive drifting simulation is shown in Figure 2(a-b,d-e). As particles with shorter tracking times have a shorter dispersal distance, the LDD decreases by an average of 47% for all sites when nearshore retention is applied to the passive drifting simulation. For the same reason, the number particles in the source zones where recruitment sites are located increases when nearshore retention is applied to the passive drifting simulation. As a results, the pattern of SZS changes for all sites from being more evenly spread throughout the 9 source zones (Figure 2(g,j)) to being dominated by the zone where the recruitment site is located (Figure 2(h,k)). In the zone where the recruitment sites is located, the SZS increases by an average of 44% for all sites.

When DVM is included in a simulation, particle dispersal changes as new particle tracks are produced and as function of recruitment site location. Compared to the passive drifting simulation, DVM decreases particle dispersal for the SBC mainland sites of Gaviota, Elwood, and Stearns, which results in a decrease in the LDD by an average of 82% for these sites. The decrease in particle dispersal for the Gaviota site can be seen in Figure 2(a,c). The long residence times and containment by the topography in the SBC appears to limit particle dispersal for particle tracks with DVM versus those with passive drifting for the SBC mainland sites. This decrease in particle dispersal produces an increase in particle concentrations near the SBC mainland sites and an increase in SZS by an average of 46% in Zone 1 where the recruitment sites are located, a similar result as nearshore retention. In contrast, DVM increases particle dispersal for the Scripps site compared to passive drifting, which results in an increase in LDD by an average of 20%. This increases particle dispersal with DVM appears to be driven by the open coastline and short retention times of the southern SC Bight. The increase in particle dispersal for the Scripps site can be seen in Figure 2(d,f). For the Scripps site, the increase in particle dispersal from DVM decreases the SZS for the Zone 7 where the Scripps site is located by an average of 16% and increases the SZS for Zones 6 and 8, which are adjacent to Zone7, by an average of 5% and 6% respectively. Unlike the other recruitment sites, the Anacapa site shows similar particle dispersal and consequently LDD and SZS for passive drifting and DVM simulations. Compared to the other recruitment sites, the circulation in the region of the Anacapa Island, where the Anacapa site is located, has the lowest velocities and shallowest bathymetry, which may be restricting particle dispersal regardless of the larval behavior.

The high sensitivity of LDD and SZS to nearshore retention and larval behavior have important implications for the use of larval connectivity calculated from biophysical models for scientific research as well as policy decisions for environmental protection (Cowen and Sponaugle 2009; Metaxas and Saunders 2009; Swearer et al. 2019). These results show that selection of larval life history parameters can dramatically change the location of predicted larval source sites by 100s of kilometers. Thus, larval connectivity predictions that are based on a single set of larval life history parameters could provide misleading information for policy decisions, such as those for marine protected areas. For this reason, our study shows the importance of sensitivity studies for larval life history parameters and validating larval transport and connectivity with field observations, such as larval recruitment.

The ocean conditions representing temperature, $T_L$ and $T_S$, show the lowest sensitivity to nearshore retention and larval behavior. $T_L$ is calculated from particle tracks and OCM temperature, while $T_S$ is calculated from SZS and OCM temperature. Although both nearshore retention and larval behavior produce significant changes in particle dispersal, temperature is relatively consistent over the horizontal scale of the changes in particle dispersal. This can be seen by comparing the areas of high particle concentrations in the mean PDMs (Figure 2(a-f)) with the mean temperature for the recruitment and reproductive periods in Figure 5(b,c)). As a result, RMSD for $T_L$ and $T_S$ for all recruitment sites is relatively small, ranging from 0.49-0.99°C and 0.31-1.1°C respectively for the simulation pairs comparing passive drifting with and without nearshore retention and passive drifting and DVM20 without nearshore retention. It is important to note that although the RMSD for $T_L$ and $T_S$ are small relative to their absolute

values, a difference of ~1°C could have be important if the temperature is near a threshold that is detrimental for larval development or survival.

The ocean condition representing food supply, Chl, shows higher sensitivity than $T_L$ and $T_S$ and lower sensitivity than SZS and LDD for all recruitment sites. Chl is calculated directly from particle tracks and surface chlorophyll from satellite data. The highest overall sensitivity for Chl comes from the Gaviota, Ellwood, and Stearns sites for simulation pair comparing passive drifting to DVM20 without nearshore retention. As the highest Chl in the SC Bight is confined to the SBC (Figure 5(a)), Chl will increase when DVM limits particle dispersal to the SBC region for Gaviota, Ellwood, and Stearns sites (Figure 2(c)). In contrast, Chl will be much less sensitive to changing particle dispersal in southern SC Bight where Chl is low throughout the region.

In summary, the higher sensitivity of LDD and SZS to nearshore retention and larval behavior than $T_L$, $T_S$, and Chl (trend 1) appears to be driven by the fact that circulation and subsequently particle dispersal in the SC Bight are much more horizontally variable than temperature and surface chlorophyll. As LDD and SZS are derived directly from particle tracks driven by circulation, they are more sensitive to the spatial changes in circulation than $T_L$, $T_S$, and Chl, which are derived from particle tracks and temperature and surface chlorophyll. All ocean conditions show similar levels of sensitivity for the SBC mainland sites of Gaviota, Ellwood, and Stearns (trend 2). This trend appears to be driven by the strong consistent circulation in the SBC. When nearshore retention or DVM is included in the simulation for the SBC mainland sites, the circulation creates a region of high particle concentrations in the SBC, which produces similar changes in ocean conditions for all three recruitment sites. Due to the variable circulation and retention near the Anacapa and Scripps sites, the addition of nearshore

retention or DVM to the simulation for these sites does not produce changes in ocean conditions consistent with the other recruitment sites. All ocean conditions appear to be the most sensitive to the two simulation pairs comparing passive drifting without retention to passive drifting with retention and to DVM20 without retention (trend 3). This result is driven by changes in particle dispersal, which are much greater when nearshore retention or DVM is added to simulations with passive drifting behavior and no nearshore retention than when both simulations have nearshore retention and/or DVM behavior.

*4.2 Identifying the ocean conditions that drive of larval recruitment*

Circulation, food supply, and temperature are discussed as potential drivers of larval recruitment of purple sea urchins in the SC Bight. Ocean conditions are considered potential drivers of interannual changes in larval recruitment if a strong correlation is found between the ocean condition and the larval recruitment index for one or more simulations and recruitment sites. We found that $T_S$ had the strongest correlation for all simulations, LDD and SZS had the second strongest correlation for a subset of simulations, and Chl and $T_L$ had no correlation for all simulations.

The ocean conditions representing circulation, LDD and SZS, displayed both weak and strong correlations with the larval recruitment index depending on the simulation. The simulations with the strongest correlations for LDD and SZS include DVM and/or nearshore retention. For these strongly correlated simulations, LDD is found to be inversely proportional to the larval recruitment index for all recruitment sites, which implies that larval dispersal occurs over a smaller area in the good recruitment years than in the poor recruitment years. For SZS, the strongly correlated simulations show that a higher percentage of larvae come from the

zones containing and adjacent to the recruitment site in the good recruitment years than the poor recruitment years. From these results, we hypothesize that circulation in the SC Bight is different between the good versus poor recruitment years, but that larval recruitment is only connected to the circulation when the larvae have behavior, such as DVM, that limits their dispersal to the region near the recruitment sites. Although this study only compares passive drifting to two simple DVM patterns, urchin larvae in the SC Bight may performing a different type of behavior that also reduces larval dispersal.

Chl is used as a proxy for larval food supply in the SC Bight because it represents amount of phytoplankton present, which is food source for sea urchin larvae. The correlation between Chl and the recruitment index is very low and inconsistent in both magnitude and sign across all simulations, implying that Chl is not driving the interannual changes in larval recruitment. For all sites, the lowest values of Chl occur during both a very high recruitment year (2000) and a very low recruitment years (1998), implying that larvae are not food limited in the SC Bight even in years with lower primary production. It is important to note that of the five ocean conditions studied, Chl has the most uncertainty as it is based on surface chlorophyll and does not account for vertical changes chlorophyll.

In prior work, Okamoto et al. (2020) analyzed 27-year larval recruitment datasets of purple sea urchins in the northern and southern SC Bight and found that recruitment was negatively correlated with sea surface temperature at the recruitment sites and positively correlated with the multivariate ENSO index (MEI), which tracks El Niño and La Niña events in the Pacific Ocean. Throughout the SC Bight, high temperatures and El Niño events were observed to correspond with low larval recruitment. Okamoto et al. (2020) found that

recruitment was highly synchronous within the northern and southern SC Bight regions, implying that recruitment was being driven by regional trends in oceanography and not by local conditions at the recruitment sites.

The ocean conditions that represent temperature are $T_L$ and $T_S$. Although Okamoto et al (2020) found that sea surface temperature was a linearly correlation with larval recruitment, $T_L$ and $T_S$ show extremely different correlations. $T_L$ is not correlated with the larval recruitment index for all sites and simulations, while $T_S$ shows a very strong correlation with the larval recruitment index for all sites and simulations. These results imply that $T_S$ is likely driving the interannual changes in larval recruitment, but $T_L$ is not. To understand why $T_L$ and $T_S$ produce divergent results, $T_L$ and $T_S$ are compared to documented thresholds for larval survival and reproduction for the purple sea urchin in the SC Bight.

In the SC Bight, the threshold temperature for lethal conditions of purple sea urchin larvae is ~18°C (Mustermann et al. 2025). $T_L$ for all simulations and recruitment sites is below this lethal threshold of 18°C. For the modeling period of 1996-2013, the highest recorded temperatures in the SC Bight occurred during a 1997-1998 El Niño event (Lynn and Bograd 2002; McClatchie et al. 2016). However, during the 1998 recruitment period, $T_L$ did not come close to the lethal level during this time with maximum $T_L$ of 15.9°C for all simulations and recruitment sites. Figure 8 shows the mean seasonal temperature cycle at the Gaviota and Scripps recruitment sites using temperatures from the OCM averaged over the 18-year modeling period. These recruitment sites represent temperature extremes in SC Bight with Gaviota in the cool northern region and Scripps in the warm southern region. The recruitment period of March through June shows mean monthly temperatures at Gaviota ranging from 12.0-

14.3°C and Scripps ranging from 14.4-16.6°C. The dashed lines from March-June in Figure 8 represent the temperatures at Gaviota and Scripps during the 1998 El Niño event, which range from 12.9-16.6°C and show that even during a strong El Niño event, the temperatures during the recruitment period do not vary significantly from the mean annual cycle. Thus, strong El Niño events, although known for producing high temperatures, appear to have minimal effect on temperatures in the SC Bight during the recruitment period. In addition, *r* calculated between $T_L$ and MEI for the recruitment period ranges from 0.07-0.27 with a mean for 0.18 for all simulations and recruitment sites, showing that ENSO events in general are not strongly correlated with temperature in the SC Bight during the recruitment period. Since warming produced by marine heatwaves during the recruitment period does not raise $T_L$ above the lethal limit for urchin larvae, $T_L$ is most likely not driver of larval recruitment for purple sea urchins in the SC Bight.

Okamoto et al. (2025) evaluated the impact of temperature on the reproduction of purple sea urchins and found that temperatures greater than about 18°C suppressed female reproduction. For the simulations with DVM and/or nearshore retention, $T_S$ for SBC mainland displays colder values clearly below the threshold of 18°C for good recruitment years, averaging 15.5-16.3°C per simulation, and warmer values close to the threshold for the poor recruitment years, averaging 17.2-17.8°C per simulation. For Anacapa and Scripps, the difference $T_S$ between the good and poor recruitment years is smaller, which average 16.3-17.2°C and 17.6-18.4°C per simulation respectively, but still shows that the good recruitment years are colder below threshold of 18°C and the poor recruitment years are warmer near or above the threshold. These results imply that $T_S$ is a likely driver of larval recruitment and that recruitment along the

SBC mainland is more strongly tied to $T_S$ than recruitment near Anacapa Island and the southern SC Bight mainland.

The SBC mainland sites display the strongest correlation between $T_S$ and the larval recruitment index for the simulations with DVM and/or nearshore retention. DVM and nearshore retention both increase the concentrations of particles in Zone 1, where the SBC mainland sites are located, which consequently increases the SZS for Zone 1 and more heavily weights $T_S$ by the temperature close to the recruitment sites. This result implies that for the SBC mainland sites, larval sources in near the recruitment sites are more likely driving recruitment at these sites than larval sources in zones farther away from the recruitment sites. For the Anacapa and Scripps sites, the inclusion of DVM and nearshore retention in the simulations did not produce a higher correlation between $T_S$ and the larval recruitment index. As DVM and nearshore retention did not produce consistently higher concentrations of particles near the Anacapa and Scripps sites, this suggests that the larval sources in the zone nearest these sites are not more important in driving larval recruitment than the larval sources in zones farther from these sites.

Okamoto et al. (2020) also found that the larval recruitment index correlated strongly with MEI. To explore this correlation, *r* is calculated for $T_S$ and mean MEI for the reproductive period. $T_S$ and mean MEI are found have a strong positive linear relationship with *r* ranging from 0.63-0.82 with a mean of 0.81 for all simulations and sites. These results suggests that El Niño events, represented by a positive MEI, are correlated with high $T_S$ and poor recruitment. The strongest El Niño event of the modeling period occurred from July 1997 to June 1998 with a mean MEI of 2.1. In Figure 8, the dashed lines from September to November represent the

temperatures at the Gaviota and Scripps sites during the 1997 reproductive period and show that the temperatures in the SC Bight were significantly higher than the annual average. Figure 9(a) shows the larval recruitment index as a function of $T_S$ versus MEI for the simulation with passive drifting, nearshore retention, and a static PLD for all recruitment sites. The data in Figure 9(a) suggests that $T_S$ greater than ~17.5°C and MEI greater than ~-0.5 are likely to produce low larval recruitment. Figure 9(b) shows the larval recruitment index as a function of $T_S$ versus SZS for the zones that are nearest the recruitment size for the simulation with DVM20, no nearshore retention, and a static PLD for all recruitment sites. The data in Figure 9(b) suggests that for good recruitment, $T_S$ is less than ~17°C, and the SZS for the zones nearest the recruitment site is greater than ~60%. In Figure 9(b), 1998 for the SBC mainland sites is an outlier as it is a poor recruitment year, but shows high SZS for the zones near the recruitment sites. $T_S$ in 1997 is the highest temperature of the 18-yr modeling period, ranging from 18.3-19.5°C, and the only year where $T_S$ does not decrease over the reproductive period. Thus for 1998, we hypothesize that although the circulation in the SBC correlated with good recruitment, the high temperatures during the 1997 reproductive period reduced larval supply in 1998 to the extent that circulation is no longer a factor in recruitment.

In summary, $T_S$ is hypothesized to be a primary driver of the interannual variation in larval recruitment of purple sea urchins in the SC Bight. Our results suggest that mean $T_S$ over the three-month reproductive period greater than 17-18°C produces poor recruitment by suppressing reproduction in adult sea urchins at the source sites, which is supported by experimental data from Okamoto et al. (2025). Circulation, through LDD and SZS, is found to be a potential driver of larval recruitment if the larvae have behavior that allows them to remain

within an average distance of ~25 km from a recruitment site in the SBC and an average distance of ~100 km from a recruitment site in the southern SC Bight. As $T_S$ also had a stronger correlation with larval recruitment for the simulations that included larval life history parameters that limited dispersal distance, we hypothesize that urchin larvae in the SC Bight are likely behaving in a way which reduces their dispersal distance and consequently that urchin larvae are more likely to come from sources near the recruitment sites. According to Swearer et al. (2019), more than half the studies published over the past 15 years used passive drifting behavior with no species-defining larval life history and the many of the remaining studies used only one larval life history trait. As much of the larval life history of marine species is unknown, our study shows that testing the sensitivity of biophysical models to larval life history parameters can help determine which parameters most influence the results and should be further studied.

In addition, we found that $T_S$ during the reproductive period of September to November is likely an important driver of larval recruitment but $T_L$ during the recruitment period of March to June is not, even in years with strong El Nino events. This suggests that the timing of species recruitment and reproduction is a critical factor in predicting the impact of temperature on larval recruitment. Also, we hypothesize that marine heatwaves which occur during time of year when temperatures are at their annual maximum are more likely to produce temperatures high enough to negatively impact recruitment and reproduction than those which occur during the time of year when temperatures are at their annual minimum. Species that recruit or reproduce during the time of year when the system temperatures are at their annual maximum are more susceptible to marine heat waves than those that recruit or reproduce at other times of the

year. As the frequency of marine heatwaves increase (Sydeman et al. 2014; Di Lorenzo and Mantua 2016; Bograd et al. 2023), understanding the relationship between the timing of marine heatwaves and species recruitment and reproduction becomes even more important.

**Acknowledgements**

This research was supported by the National Science Foundation Biological Oceanography Program (OCE-2023693).

**References**

Bandara, K., Ø. Varpe, L. Wijewardene, V. Tverberg, and K. Eiane. 2021. Two hundred years of zooplankton vertical migration research. Biol. Rev. **96**: 1547–1589. doi:10.1111/brv.12715

Bell, T. W., K. C. Cavanaugh, D. C. Reed, and D. A. Siegel. 2015. Geographical variability in the controls of giant kelp biomass dynamics. J. Biogeogr. **42**: 2010–2021. doi:10.1111/jbi.12550

Bograd, S. J. and others. 2023. Climate change impacts on Eastern Boundary Upwelling Systems. Ann Rev Mar Sci **15**: 303–328. doi:10.1146/annurev-marine-032122-021945

Botsford, L. W., S. R. Wing, and J. L. Largier. 1998. Population dynamics and management implications of larval dispersal. South Afr. J. Mar. Sci. **19**: 131–142. doi:10.2989/025776198784126845

Brokaw, R. J., D. A. Siegel, and L. Washburn. 2024. Physical Drivers of Surface Water Retention in the Santa Barbara Channel. J. Geophys. Res. Oceans **129**: e2024JC021246. doi:10.1029/2024JC021246

Cohen, J. H., and R. B. Forward. 2009. Zooplankton diel vertical migration — a review of proximate control, p. 77–110. *In* J.D.M. Gordon, R.J.A. Atkinson, and R.N. Gibson [eds.], Oceanography and marine biology: an annual review: Volume 47. Taylor & Francis.

Cowen, R. K., and S. Sponaugle. 2009. Larval dispersal and marine population connectivity. Annu Rev Mar Sci **1**: 443–466. doi:10.1146/annurev.marine.010908.163757

Di Lorenzo, E., and N. Mantua. 2016. Multi-year persistence of the 2014/15 North Pacific marine heatwave. Nat. Clim. Change **6**: 1042–1047. doi:10.1038/nclimate3082

Doll, P. C., C. F. Caballes, A. S. Hoey, S. Uthicke, S. D. Ling, and M. S. Pratchett. 2022. Larval Settlement in Echinoderms: A Review of Processes and Patterns, p. 433–494. *In* Oceanography and Marine Biology: An Annual Review, Volume 60. CRC Press.

Doney, S. C. and others. 2012. Climate Change Impacts on Marine Ecosystems. Annu. Rev. Mar. Sci. **4**: 11–37. doi:10.1146/annurev-marine-041911-111611

Dong, C. M. and others. 2012. Three-dimensional oceanic eddy analysis in the Southern California Bight from a numerical product. J. Geophys. Res.-Oceans **117**. doi:10.1029/2011jc007354

Dong, C. M., E. Y. Idica, and J. C. McWilliams. 2009. Circulation and multiple-scale variability in the Southern California Bight. Prog. Oceanogr. **82**: 168–190. doi:10.1016/j.pocean.2009.07.005

Dong, C. M., and J. C. McWilliams. 2007. A numerical study of island wakes in the Southern California Bight. Cont. Shelf Res. **27**: 1233–1248. doi:10.1016/j.csr.2007.01.016

Dong, C. M., J. C. McWilliams, A. Hall, and M. Hughes. 2011. Numerical simulation of a synoptic event in the Southern California Bight. J. Geophys. Res.-Oceans **116**: C05018. doi:10.1029/2010jc006578

Estes, J. A., and D. O. Duggins. 1995. Sea Otters and Kelp Forests in Alaska: Generality and Variation in a Community Ecological Paradigm. Ecol. Monogr. **65**: 75–100. doi:10.2307/2937159

Filbee-Dexter, K., and R. Scheibling. 2014. Sea urchin barrens as alternative stable states of collapsed kelp ecosystems. Mar. Ecol. Prog. Ser. **495**: 1–25. doi:10.3354/meps10573

Hagerty, M., N. Reyns, and J. Pineda. 2018. Constrained nearshore larval distributions and thermal stratification. Mar. Ecol. Prog. Ser. **595**: 105–122. doi:10.3354/meps12561

Henderikx Freitas, F., D. A. Siegel, S. Maritorena, and E. Fields. 2017. Satellite assessment of particulate matter and phytoplankton variations in the Santa Barbara Channel and its surrounding waters: Role of surface waves. J. Geophys. Res. Oceans **122**: 355–371. doi:10.1002/2016JC012152

Hickey, B. M. 1993. Chapter 2. Physical Oceanography, p. 19–70. *In* M.D. Dailey, D.J. Reish, and J.W. Anderson [eds.], Ecology of the Southern California Bight. University of California Press.

Kahru, M., R. M. Kudela, C. R. Anderson, and B. G. Mitchell. 2015. Optimized merger of ocean chlorophyll algorithms of MODIS-Aqua and VIIRS. IEEE Geosci. Remote Sens. Lett. **12**: 2282–2285. doi:10.1109/LGRS.2015.2470250

Kahru, M., R. M. Kudela, M. Manzano-Sarabia, and B. Greg Mitchell. 2012. Trends in the surface chlorophyll of the California Current: Merging data from multiple ocean color satellites. Deep Sea Res Part II Top Stud Ocean. **77–80**: 89–98. doi:10.1016/j.dsr2.2012.04.007

Lafferty, K. D. 2004. Fishing for lobsters indirectly increases epidemics in sea urchins. Ecol. Appl. **14**: 1566–1573. doi:10.1890/03-5088

Lynn, R. J., and S. J. Bograd. 2002. Dynamic evolution of the 1997–1999 El Niño–La Niña cycle in the southern California Current System. Prog. Oceanogr. **54**: 59–75. doi:10.1016/S0079-6611(02)00043-5

Lynn, R. J., and J. J. Simpson. 1987. The California Current system: The seasonal variability of its physical characteristics. J. Geophys. Res. **92**: 12947. doi:10.1029/JC092iC12p12947

Mann, K. H., and P. A. Breen. 1972. The Relation Between Lobster Abundance, Sea Urchins, and Kelp Beds. J. Fish. Res. Board Can. **29**: 603–605. doi:10.1139/f72-104

McClatchie, S., M. G. Jacox, M. D. Ohman, L. M. Sala, and R. Goericke. 2016. State of the California Current 2015–16: Comparisons with the 1997–98 El Nino. Calif. Coop. Fish. Invest. Rep. **57**: 5–61.

Metaxas, A. 2020. Larval ecology of echinoids, p. 77–93. *In* Developments in Aquaculture and Fisheries Science. Elsevier.

Metaxas, A., and M. Saunders. 2009. Quantifying the “Bio-” components in biophysical models of larval transport in marine benthic invertebrates: advances and pitfalls. Biol. Bull. **216**: 257–272. doi:10.2307/25548159

Mitarai, S., D. A. Siegel, J. R. Watson, C. Dong, and J. C. McWilliams. 2009. Quantifying connectivity in the coastal ocean with application to the Southern California Bight. J. Geophys. Res.-Oceans **114**: C10026. doi:10.1029/2008JC005166

Morgan, S. G. 2001. The larval ecology of marine communities, p. 159–181. *In* M.D. Bertness, S.D. Gaines, and M.E. Hay [eds.], Marine community ecology. Sinauer Associates.

Morgan, S. G., J. L. Fisher, S. H. Miller, S. T. McAfee, and J. L. Largier. 2009. Nearshore larval retention in a region of strong upwelling and recruitment limitation. Ecology **90**: 3489–3502. doi:10.1890/08-1550.1

Morgan, S. G., S. H. Miller, M. J. Robart, and J. L. Largier. 2018. Nearshore Larval Retention and Cross-Shelf Migration of Benthic Crustaceans at an Upwelling Center. Front. Mar. Sci. **5**: 161. doi:10.3389/fmars.2018.00161

Mustermann, M. J., S. Karelitz, R. Ferraro, L. Rogers-Bennett, R. D. Simons, and D. K. Okamoto. 2025. Food limitation erodes the thermal tolerance of larvae in an ecosystem engineer. Ecology **In Review**.

Myers, R. A. 1998. When do environment–recruitment correlations work? Rev. Fish Biol. Fish. **8**: 285–305. doi:10.1023/A:1008828730759

Nishimoto, M. M., R. D. Simons, and M. S. Love. 2019. Offshore oil production platforms as potential sources of larvae to coastal shelf regions off southern California. Bull. Mar. Sci. **95**: 535–558. doi:10.5343/bms.2019.0033

Ohlmann, J. C., and S. Mitarai. 2010. Lagrangian assessment of simulated surface current dispersion in the coastal ocean. Geophys. Res. Lett. **37**: L17602. doi:10.1029/2010GL044436

Okamoto, D. K., S. C. Schroeter, and D. C. Reed. 2020. Effects of ocean climate on spatiotemporal variation in sea urchin settlement and recruitment. Limnol. Oceanogr. **65**: 2076–2091. doi:10.1002/lno.11440

Okamoto, D. K., N. B. Spindel, B. Collicutt, M. J. Mustermann, S. Karelitz, and Gimenez. 2025. Thermal suppression of gametogenesis explains historical collapses in larval recruitment. Ecology **In Review**.

Otero, M., and D. Siegel. 2004. Spatial and temporal characteristics of sediment plumes and phytoplankton blooms in the Santa Barbara Channel. Deep Sea Res. Part II Top. Stud. Oceanogr. **51**: 1129–1149. doi:10.1016/S0967-0645(04)00104-3

Page, H. 2019. Distribution and potential larval connectivity of the non-native Watersipora (Bryozoa) among harbors, offshore oil platforms, and natural reefs. Aquat. Invasions **14**: 615–637. doi:10.3391/ai.2019.14.4.04

Paris, C., L. Chérubin, and R. Cowen. 2007. Surfing, spinning, or diving from reef to reef: effects on population connectivity. Mar. Ecol. Prog. Ser. **347**: 285–300. doi:10.3354/meps06985

Pineda, J., J. Hare, and S. Sponaugle. 2007. Larval transport and dispersal in the coastal ocean and consequences for population connectivity. Oceanogr **20**: 22–39. doi:10.5670/oceanog.2007.27

Pineda, J., F. Porri, V. Starczak, and J. Blythe. 2010. Causes of decoupling between larval supply and settlement and consequences for understanding recruitment and population connectivity. J. Exp. Mar. Biol. Ecol. **392**: 9–21. doi:10.1016/j.jembe.2010.04.008

Rogers-Bennett, L., and C. A. Catton. 2019. Marine heat wave and multiple stressors tip bull kelp forest to sea urchin barrens. Sci. Rep. **9**: 15050. doi:10.1038/s41598-019-51114-y

Rogers-Bennett, L., and D. Okamoto. 2020. Mesocentrotus franciscanus and Strongylocentrotus purpuratus, p. 593–608. *In* Developments in Aquaculture and Fisheries Science. Elsevier.

Schroeter, S. C., J. D. Dixon, T. Ebert, and J. Richards. 2017. SBC LTER: Time series of settlement of urchins and other invertebrates.doi:10.6073/PASTA/A7BA12263D75BE25CE526A2E20B0E6F3

Shanks, A. L. and others. 2020. Marine heat waves, climate change, and failed spawning by coastal invertebrates. Limnol. Oceanogr. **65**: 627–636. doi:10.1002/lno.11331

Simons, R. D., and D. Catlett. 2023. Regulation of a surface chlorophyll hotspot by wind-driven upwelling and eddy circulation in the Santa Barbara Channel, Southern California. Prog. Oceanogr. **217**: 103096. doi:10.1016/j.pocean.2023.103096

Simons, R. D., M. M. Nishimoto, L. Washburn, K. S. Brown, and D. A. Siegel. 2015. Linking kinematic characteristics and high concentrations of small pelagic fish in a coastal mesoscale eddy. Deep Sea Res Part Ocean. Res Pap. **100**: 34–47. doi:10.1016/j.dsr.2015.02.002

Simons, R. D., H. M. Page, S. Zaleski, R. Miller, J. E. Dugan, D. M. Schroeder, and B. Doheny. 2016. The effects of anthropogenic structures on habitat connectivity and the potential spread of non-native invertebrate species in the offshore environment M. (Gee) G. Chapman [ed.]. PLOS ONE **11**: e0152261. doi:10.1371/journal.pone.0152261

Simons, R. D., D. A. Siegel, and K. S. Brown. 2013. Model sensitivity and robustness in the estimation of larval transport: A study of particle tracking parameters. J. Mar. Syst. **119**: 19–29. doi:10.1016/J.Jmarsys.2013.03.004

Stige, L., M. Hunsicker, K. Bailey, N. Yaragina, and J. Hunt GL. 2013. Predicting fish recruitment from juvenile abundance and environmental indices. Mar. Ecol. Prog. Ser. **480**: 245–261. doi:10.3354/meps10246

Swearer, S. E., E. A. Treml, and J. S. Shima. 2019. A Review of Biophysical Models of Marine Larval Dispersal, p. 325–356. *In* S.J. Hawkins, A.L. Allcock, A.E. Bates, L.B. Firth, I.P. Smith, S.E. Swearer, and P.A. Todd [eds.], Oceanography and Marine Biology. CRC Press.

Sydeman, W. J., M. García-Reyes, D. S. Schoeman, R. R. Rykaczewski, S. A. Thompson, B. A. Black, and S. J. Bograd. 2014. Climate change and wind intensification in coastal upwelling ecosystems. Science **345**: 77–80. doi:10.1126/science.1251635

Tegner, M., and P. Dayton. 1991. Sea urchins, El Ninos, and the long term stability of Southern California kelp forest communities. Mar. Ecol. Prog. Ser. **77**: 49–63. doi:10.3354/meps077049

Underwood, A. J., and M. J. Keough. 2001. Supply-side ecology: the nature and consequences of variations in recruitment of intertidal organisms, p. 183–200. *In* M.D. Bertness, S.D. Gaines, and M.E. Hay [eds.], Marine community ecology. Sinauer Associates.

Watson, J. R., S. Mitarai, D. A. Siegel, J. E. Caselle, C. Dong, and J. C. McWilliams. 2010. Realized and potential larval connectivity in the southern California bight. Mar Ecol Prog Ser **401**: 31–48. doi:10.3354/meps08376

White, J. W. and others. 2019. Connectivity, Dispersal, and Recruitment: Connecting Benthic Communities and the Coastal Ocean. Oceanography **32**: 50–59. doi:10.5670/oceanog.2019.310

Winant, C. D., E. P. Dever, and M. C. Hendershott. 2003. Characteristic patterns of shelf circulation at the boundary between central and southern California. J. Geophys. Res. Oceans **108**: 3021. doi:10.1029/2001JC001302

Yamhure, G. M., N. Reyns, and J. Pineda. 2021. High Larval Concentrations and Onshore Transport of Barnacle Cyprids Associated With Thermal Stratification. Front. Mar. Sci. **8**: 748389. doi:10.3389/fmars.2021.748389

**Figures**

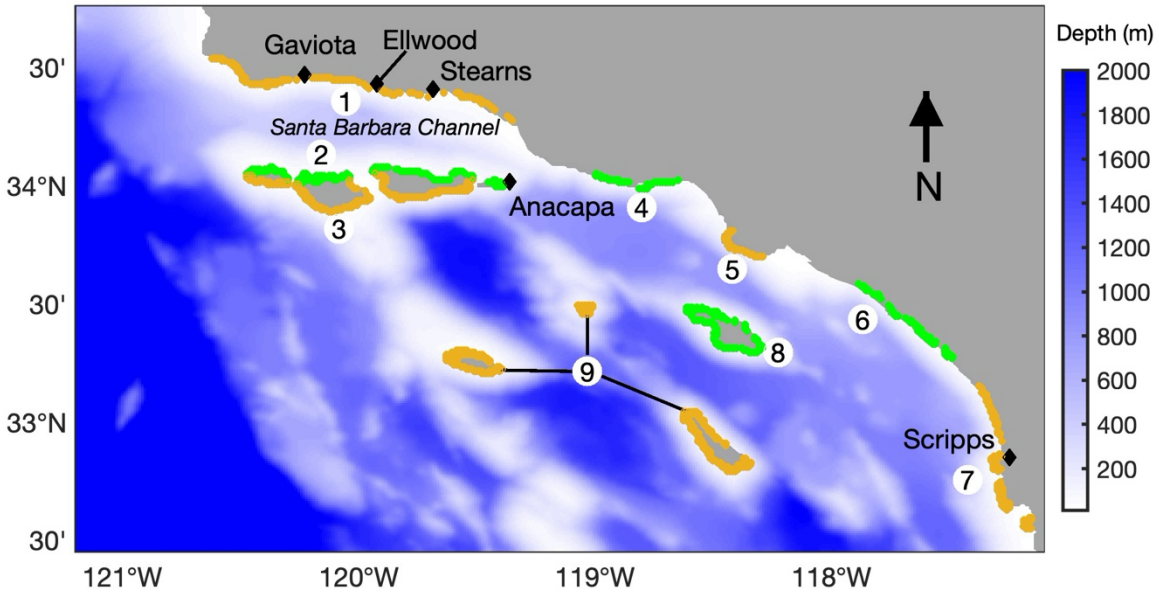


Figure 1: Southern California Bight: study area and model domain. Black diamonds are the 5 larval recruitment sites: Gaviota, Ellwood, Stearns, Anacapa, and Scripps. Green and yellow coastline locations are the nine source zones, which are identified by the black numbers: (1) mainland of the Santa Barbara Channel, (2) north side of the North Channel Islands, (3) south side of the North Channel Islands, (4-7) groups of contiguous source sites along the central and southern mainland of the Southern California Bight, (8) Catalina Island, and (9) three South Channel Islands

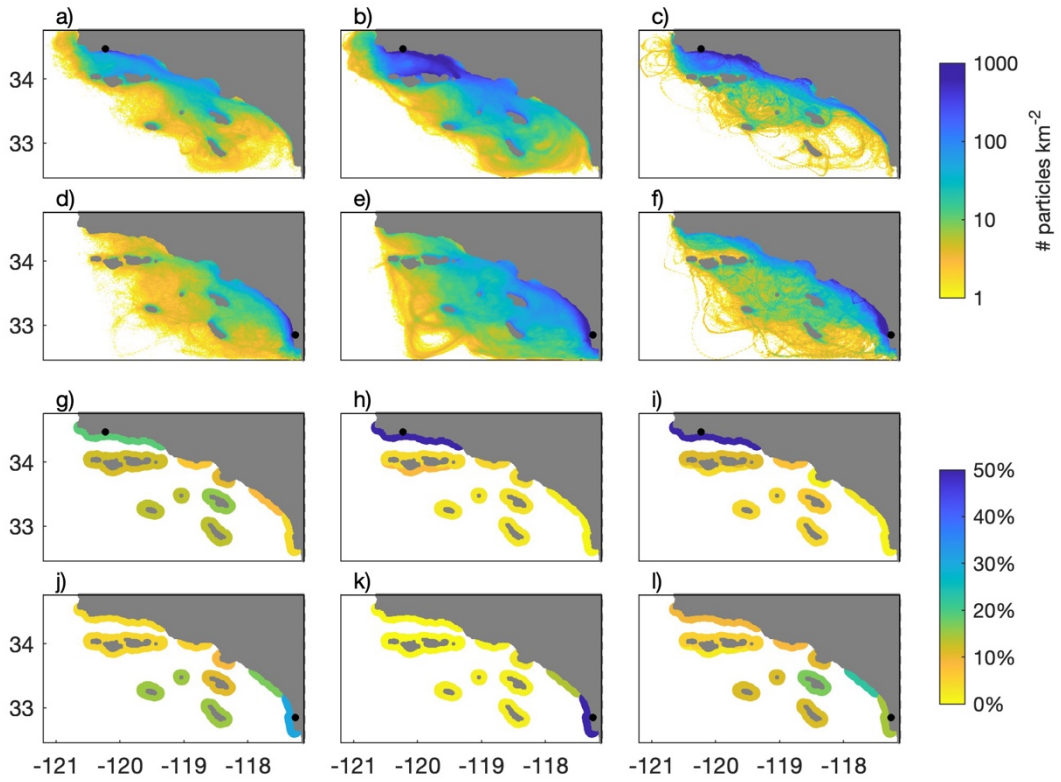


Figure 2: (a-f) Mean particle density maps (PDMs) and (g-l) mean source zone strength (SZS) for three following simulations with static PLDs: (1) passive drifting without nearshore retention for Gaviota (a,g) and for Scripps (d,j), (2) passive drifting with nearshore retention for Gaviota (b,h) and Scripps (e,k), and (3) DVM20 without nearshore retention for Gaviota (c,f) and for Scripps (f,l). PDMs and SZS have been averaged over all months of the modeling period (1996-2013). PDMs are plotted on a log scale.

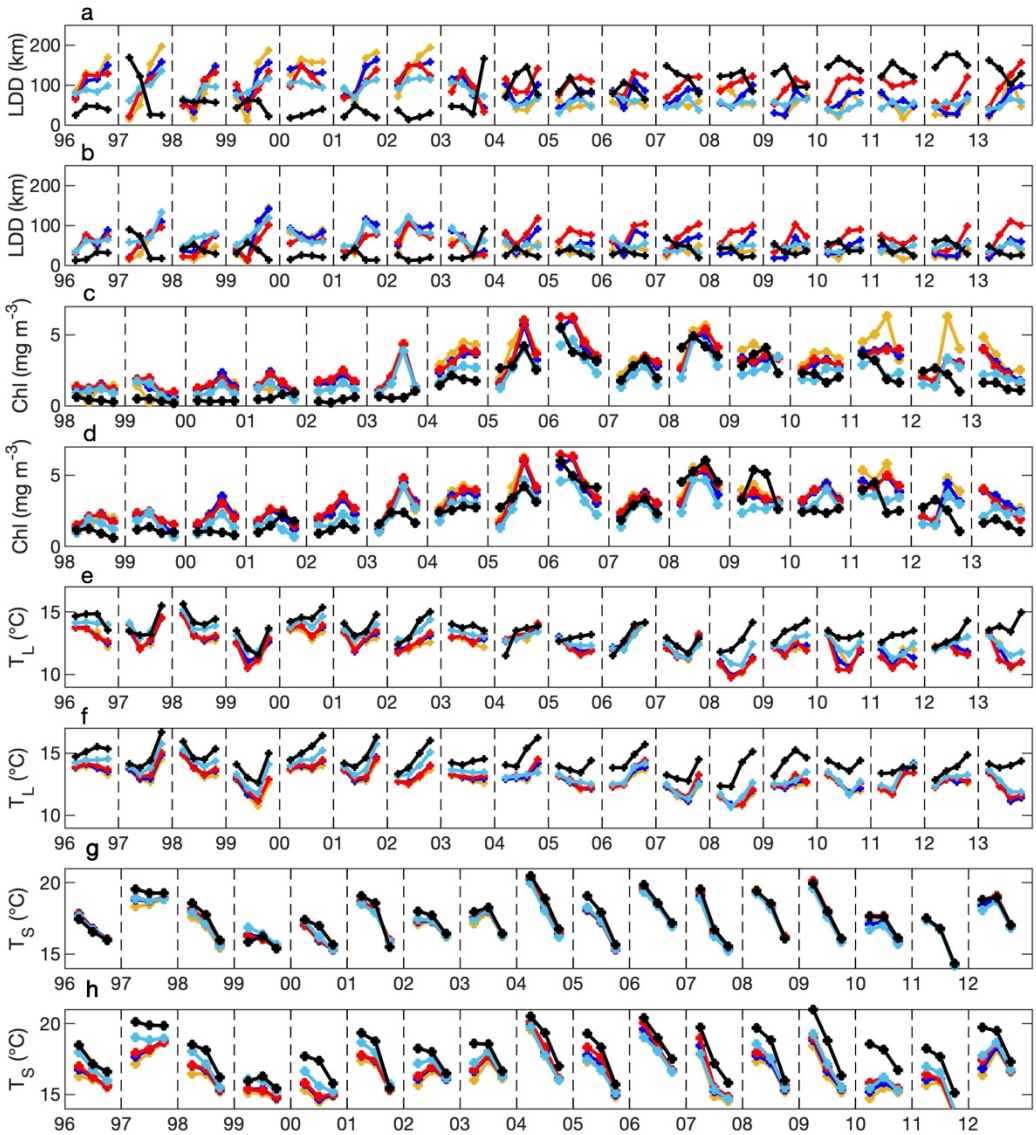


Figure 3: Ocean conditions for the simulation with passive drifting behavior, no nearshore retention, and static PLD (S1) and the simulation with passive drifting behavior, nearshore retention, and static PLD (S2): (a) LDD (km) for S1, (b) LDD (km) for S2, (c) Chl (mg $m^{-3}$) for S1, (d) Chl (mg $m^{-3}$) for S2, (e) $T_L$ (°C) for S1, (f) $T_L$ (°C) for S2, (g) $T_S$ (°C) for S1, and (h) $T_S$ (°C) for S2. LDD, Chl, and $T_L$ are shown for the larval recruitment period of March-June. $T_S$ is shown for the reproductive period of September-November. Gaviota is the yellow line. Ellwood is the dark blue line. Stearns is the red line. Anacapa is the light blue line. Scripps is the black line.

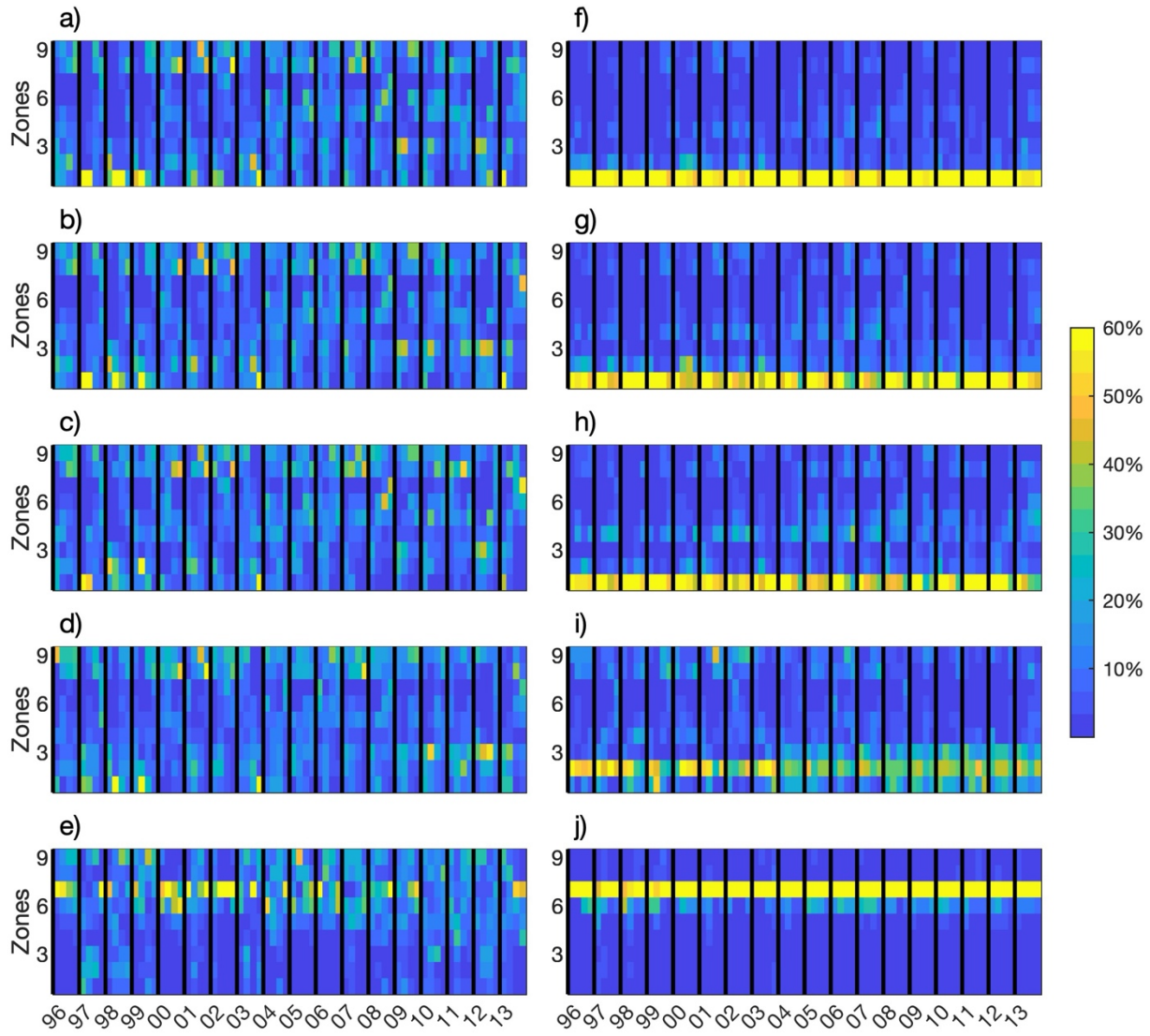


Figure 4: SZS for two simulations. The simulation with passive drifting behavior, no nearshore retention, and a static PLD for (a) Gaviota, (b) Ellwood, (c) Stearns, (d) Anacapa, and (e) Scripps, and the simulation with passive drifting behavior, nearshore retention, and a static PLD for (f) Gaviota, (g) Ellwood, (h) Stearns, (i) Anacapa, and (j) Scripps. SZS is shown for the recruitment period of March-June. Units for SZS is in percentage of particles. Zones 1-9 are shown in Figure 1.

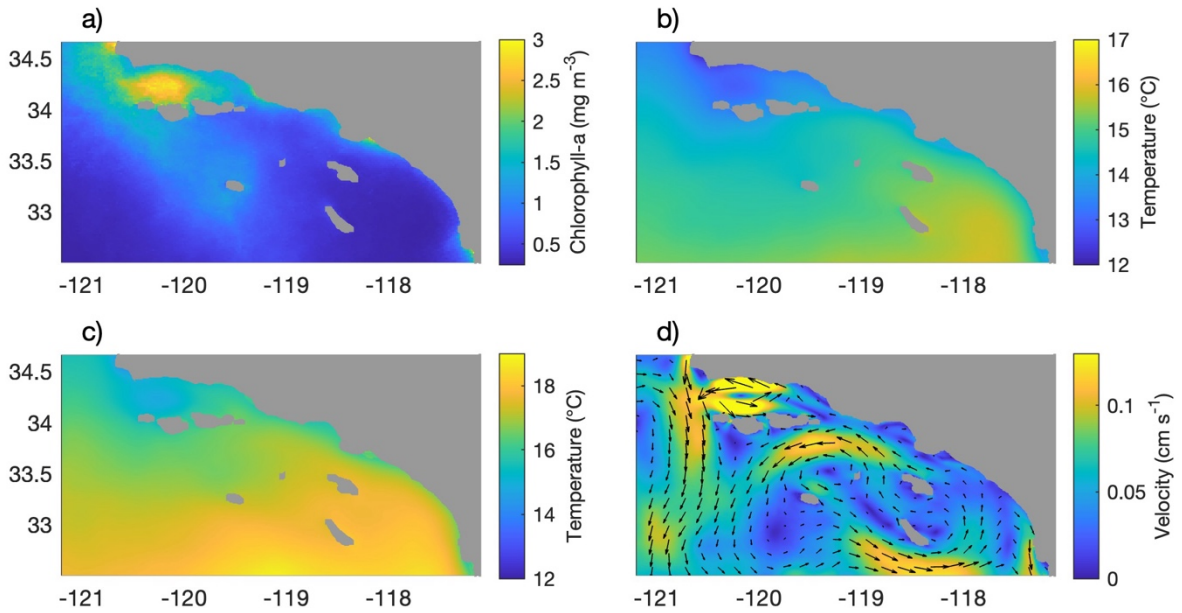


Figure 5: (a) Mean surface chlorophyll-a (mg $m^{-3}$) from satellite data for the recruitment period, (b) mean temperature (°C) averaged over top 50 m of water column for the recruitment period, (c) mean temperature (°C) averaged over top 50 m of water column for the reproductive period, and (d) mean velocity (cm $s^{-1}$) averaged over the top 50 m of the water column for the recruitment period. All data is averaged over the modeling period of 1996-2013. The recruitment period is from March to June. The reproductive period is from September to November.

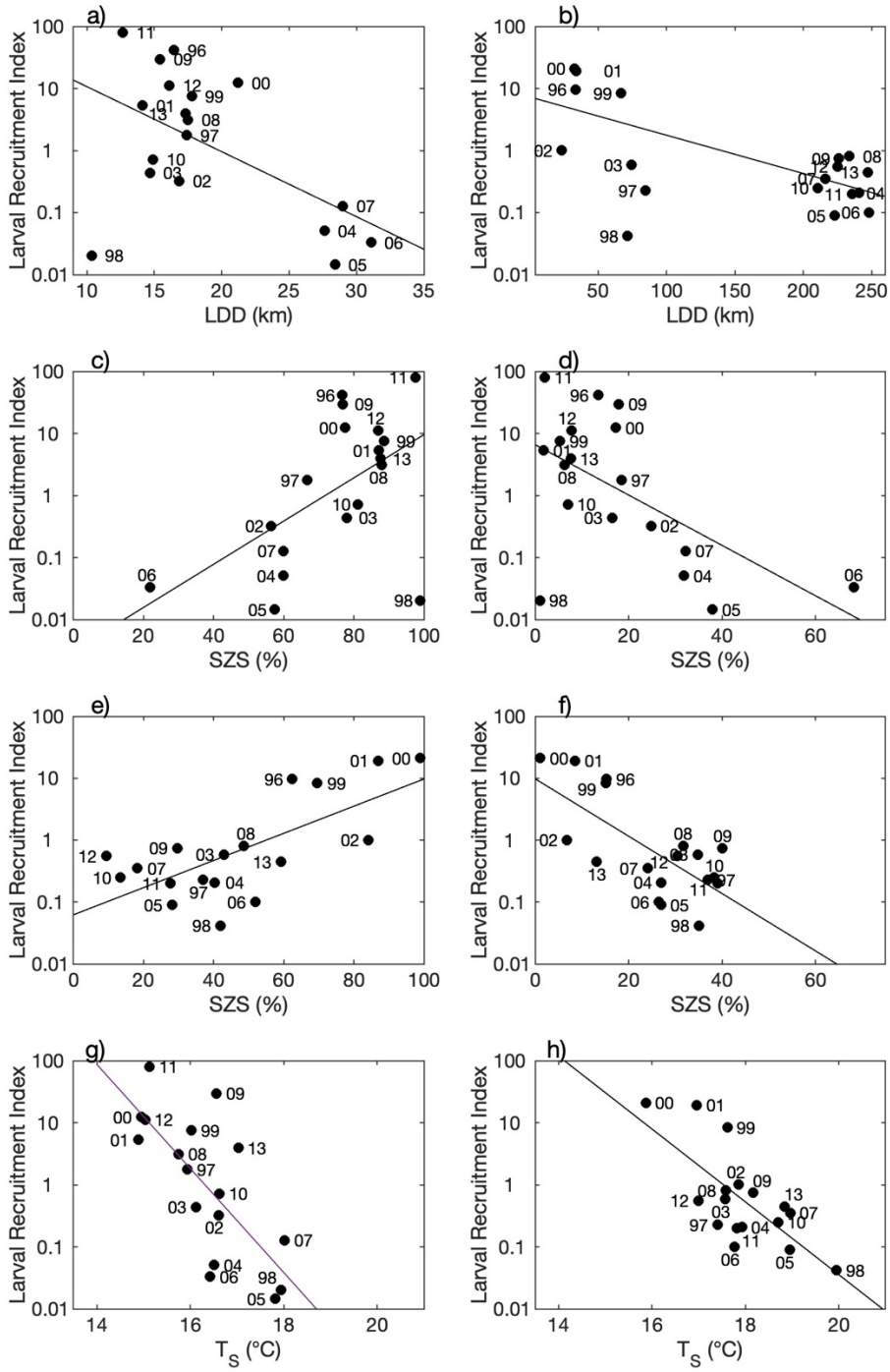


Figure 6: LDD (km) versus the larval recruitment index for the simulation with DVM40 behavior, nearshore retention, and a static PLD for (a) Gaviota and (b) Scripps. SZS (%) versus the larval recruitment index for the simulation with DVM20 behavior, no nearshore retention, and a static PLD for positive *r* for (c) Gaviota and (e) Scripps and for negative *r* for (d) Gaviota and (f) Scripps. $T_S$ (°C) versus the larval recruitment index for the simulation with passive drifting behavior, nearshore retention, and a static PLD for (g) Gaviota and (h) Scripps. Each solid black circle represents one year. The solid black line shows the linear regression for all years.

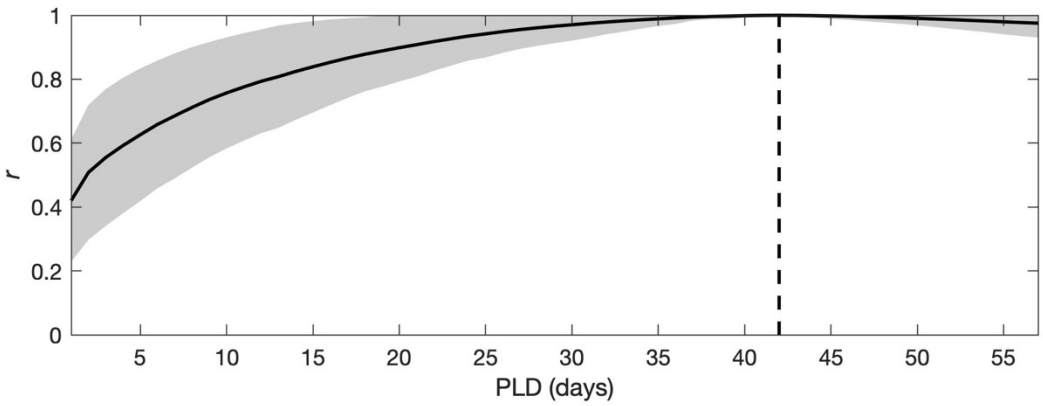


Figure 7: Pearson's *r* versus PLD (days). *r* is calculated between the particle density map (PDM) with a PLD of 42 days and the PDMs with PLDs of 1-56 days for all simulations, recruitment sites, and months of the modeling period.

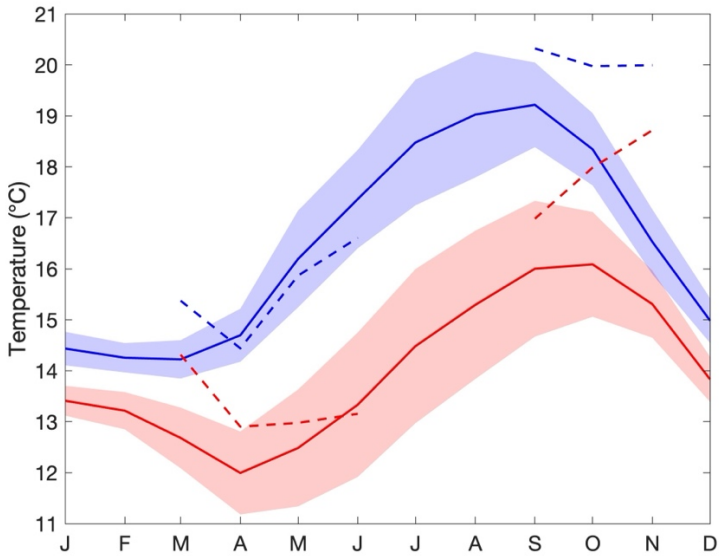


Figure 8: Mean annual temperature cycle ± 1 standard deviation (°C) at 5m depth for Gaviota (red) and Scripps (blue). Dashed lines represent the reproductive period (September-November) for 1997 and the recruitment period (March-June) for 1998. Temperature comes from the ocean circulation model and is averaged over the modeling period of 1996-2013.

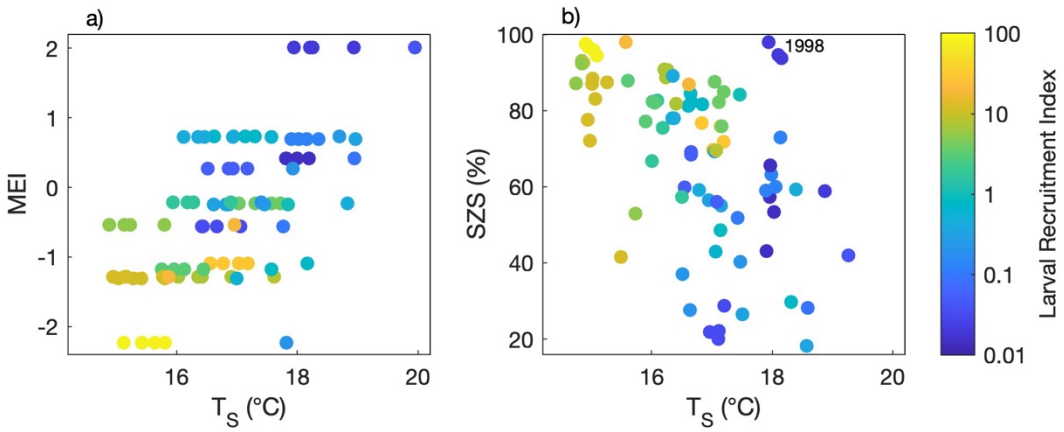


Figure 9: Larval recruitment index as a function of (a) $T_S$ (°C) and MEI for the simulation with passive drifting behavior, nearshore retention, and a static PLD and (b) $T_S$ (°C) and total SZS (%) for the three zones nearest the recruitment site for the simulation with DVM20 behavior, no nearshore retention, and a static PLD. A circle represents one year. Data from all recruitment sites are displayed.